Age Estimation of Bloodstains Using Smartphone and Digital Image Analysis

Alisa Yaodam

A Thesis Submitted in Partial Fulfillment of the Requirement for the Degree of Master of Science in Forensic Science

Prince of Songkla University

2016

Thesis Title	Age estimation of bloodstains using smartphone and digital image analysis
Author	Miss Alisa Yaodam
Major Program	Forensic Science

Major Advisor:

……..……..

(Asst. Prof. Dr. Phuvadol Thanakiatkrai)

Co-advisor

……

(Asst. Prof. Dr.Thitika Kitpipit)

Examining Committee:

……..……Chairperson

(Assoc.Pol.Maj.Gen Sant Sukhavachana)

…….....Committee

(Asst. Prof. Dr. Phuvadol Thanakiatkrai)

…….....Committee

(Asst. Prof. Dr.Thitika Kitpipit)

……Committee

(Dr. Krueawan Yoonram)

The Graduate School, Prince of Songkla University, has approved this thesis as Partial fulfillment of the requirement for the Master of Science Degree in Forensic Science.

……..…….

(Assoc. Prof. Dr. Teerapol Srichana)

Dean of Graduate School

This is to certify that the work here submitted is the result of the candidate's own investigations. Due acknowledgement has been made of any assistance received.

…….....signature
(Asst. Prof. Dr. Phuvadol Thanakiatkrai)
Major Advisor

…….....signature
(Asst. Prof. Dr. Thitika Kitpipit)
Co-advisor

…….....signature
(Alisa Yaodam)
Candidate

I hereby certify that this work has not been accepted in substance for any degree, and is not being currently submitted in candidature for any degree.

…….....signature
(Alisa Yaodam)
Candidate

Thesis Title Age estimation of bloodstains using smartphones and digital image analysis
Author Miss Alisa Yaodam
Major program Forensic Science
Academic Year 2015

ABSTRACT

The determination of bloodstain age can link the bloodstain to the crime, exclude a bloodstain as being irrelevant to the crime, approximate the time since the event has occurred, and collaborate eyewitness accounts. However, estimating the age of bloodstain is still a problem in actual forensic science practice. In this study, we used digital image analysis of bloodstains to estimate the time since deposition. This method was performed under different controlled conditions, i.e. with different donors, substrate materials, humidity, light exposure, anticoagulant and temperatures to determine the effects of each factor on the age estimation process. Three smartphones (Samsung Galaxy S Plus, Apple iPhone 4, and Apple iPad 2) were compared. The environmental effects – temperature, humidity, light exposure, and anticoagulant – on the bloodstain age estimation process were explored. The color values from the digital images were extracted and correlated with time since deposition. Magenta had the highest correlation (R^2= 0.966) and was selected for further studies. The Samsung Galaxy S Plus was the most suitable smartphone as its magenta decreased exponentially with increasing time and had highest repeatability (low variation within and between pictures). Moreover 83% of mock casework samples were correctly classified. No significant within-person and between-person variations (p >0.05) was observed. However, the camera, temperature, humidity, and substrate color were influenced the color change of magenta and thus they affected the age determination process. Further improvements to the process could be achieved by including the environmental factor in the prediction equations.

Our technique provides a cheap, rapid, easy-to-use, and truly portable alternative to more complicated analysis using specialized equipment, e.g.

spectroscopy and HPLC. With proper lighting and controls, the method has the potential to be used in crime scenes directly.

ACKNOWLEDGEMENTS

The success of this thesis could be attributed to the extensive support from many people and I would like to express my deep gratitude to all those who gave me this opportunity to complete my studies:

My special appreciation is extended to my major advisor, Asst. Prof. Dr. Phuvadol Thanakiatkrai and my co-advisor, Asst. Prof. Dr. Thitika Kitpipit, for valuable supervisions, creative guidance and encouragement throughout this thesis.

My appreciation is also extended to my examiners. Assoc. Pol. Maj. Gen Sant Sukhavachana and Dr. KrueawanYoonram for their kindness in examining the thesis and providing valuable suggestions.

I gratefully acknowledge the scholarship provided by Graduate School, Prince of Songkla University.

I would like to thanks all staff at Department of Applied Science, Faculty of Science, Prince of Songkla University for their supporting instrument.

My final words of appreciation go to my family for their unwavering support and encouragement in my educational endeavors and special thanks are extended to my friends at Department of Applied Science for their kind support.

Alisa Yaodam

CONTENTS

LIST OF TABLES

LIST OF FIGURES

LIST OF PAPERS AND MANUSCRIPTS

Thanakiatkrai, P., Yaodam, A., Kitpipit, T. 2013. Age estimation of bloodstains using smartphones and digital image analysis. Forensic Science International 233 (2013) 288-297.

ELSEVIER LICENSE
TERMS AND CONDITIONS

Mar 07, 2016

This is a License Agreement between Phuvadol Thanakiatkrai ("You") and Elsevier ("Elsevier") provided by Copyright Clearance Center ("CCC"). The license consists of your order details, the terms and conditions provided by Elsevier, and the payment terms and conditions.

All payments must be made in full to CCC. For payment instructions, please see information listed at the bottom of this form.

Supplier	Elsevier Limited The Boulevard,Langford Lane Kidlington,Oxford,OX5 1GB,UK
Registered Company Number	1982084
Customer name	Phuvadol Thanakiatkrai
Customer address	Dept. of Applied Science Hat Yai, Songkhla 90112
License number	3823520565776
License date	Mar 07, 2016
Licensed content publisher	Elsevier
Licensed content publication	Forensic Science International
Licensed content title	Age estimation of bloodstains using smartphones and digital image analysis
Licensed content author	Phuvadol Thanakiatkrai,Alisa Yaodam,Thitika Kitpipit
Licensed content date	10 December 2013
Licensed content volume number	233
Licensed content issue number	1-3
Number of pages	10
Start Page	288
End Page	297
Type of Use	reuse in a thesis/dissertation
Portion	full article
Format	both print and electronic
Are you the author of this Elsevier article?	Yes
Will you be translating?	No
Title of your thesis/dissertation	Age Estimation of Bloodstains Using Smartphone and Digital Image Analysis
Expected completion date	Apr 2016
Estimated size (number of pages)	60

Elsevier VAT number	GB 494 6272 12
Permissions price	0.00 USD
VAT/Local Sales Tax	0.00 USD / 0.00 GBP
Total	0.00 USD

Terms and Conditions

INTRODUCTION

1. The publisher for this copyrighted material is Elsevier. By clicking "accept" in connection with completing this licensing transaction, you agree that the following terms and conditions apply to this transaction (along with the Billing and Payment terms and conditions established by Copyright Clearance Center, Inc. ("CCC"), at the time that you opened your Rightslink account and that are available at any time at http://myaccount.copyright.com).

GENERAL TERMS

2. Elsevier hereby grants you permission to reproduce the aforementioned material subject to the terms and conditions indicated.
3. Acknowledgement: If any part of the material to be used (for example, figures) has appeared in our publication with credit or acknowledgement to another source, permission must also be sought from that source. If such permission is not obtained then that material may not be included in your publication/copies. Suitable acknowledgement to the source must be made, either as a footnote or in a reference list at the end of your publication, as follows:
"Reprinted from Publication title, Vol /edition number, Author(s), Title of article / title of chapter, Pages No., Copyright (Year), with permission from Elsevier [OR APPLICABLE SOCIETY COPYRIGHT OWNER]." Also Lancet special credit - "Reprinted from The Lancet, Vol. number, Author(s), Title of article, Pages No., Copyright (Year), with permission from Elsevier."
4. Reproduction of this material is confined to the purpose and/or media for which permission is hereby given.
5. Altering/Modifying Material: Not Permitted. However figures and illustrations may be altered/adapted minimally to serve your work. Any other abbreviations, additions, deletions and/or any other alterations shall be made only with prior written authorization of Elsevier Ltd. (Please contact Elsevier at permissions@elsevier.com)
6. If the permission fee for the requested use of our material is waived in this instance, please be advised that your future requests for Elsevier materials may attract a fee.
7. Reservation of Rights: Publisher reserves all rights not specifically granted in the combination of (i) the license details provided by you and accepted in the course of this licensing transaction, (ii) these terms and conditions and (iii) CCC's Billing and Payment terms and conditions.
8. License Contingent Upon Payment: While you may exercise the rights licensed immediately upon issuance of the license at the end of the licensing process for the transaction, provided that you have disclosed complete and accurate details of your proposed use, no license is finally effective unless and until full payment is received from you (either by publisher or by CCC) as provided in CCC's Billing and Payment terms and conditions. If full payment is not received on a timely basis, then any license preliminarily granted shall be deemed automatically revoked and shall be void as if never granted. Further, in the event that you breach any of these terms and conditions or any of CCC's Billing and Payment terms and conditions, the license is automatically revoked and shall be void as if never granted. Use of materials as described in a revoked license, as well as any use of the materials beyond the scope of an unrevoked license, may constitute copyright infringement and publisher reserves the right to take any and all action to protect its copyright in the materials.
9. Warranties: Publisher makes no representations or warranties with respect to the licensed

material.
10. Indemnity: You hereby indemnify and agree to hold harmless publisher and CCC, and their respective officers, directors, employees and agents, from and against any and all claims arising out of your use of the licensed material other than as specifically authorized pursuant to this license.
11. No Transfer of License: This license is personal to you and may not be sublicensed, assigned, or transferred by you to any other person without publisher's written permission.
12. No Amendment Except in Writing: This license may not be amended except in a writing signed by both parties (or, in the case of publisher, by CCC on publisher's behalf).
13. Objection to Contrary Terms: Publisher hereby objects to any terms contained in any purchase order, acknowledgment, check endorsement or other writing prepared by you, which terms are inconsistent with these terms and conditions or CCC's Billing and Payment terms and conditions. These terms and conditions, together with CCC's Billing and Payment terms and conditions (which are incorporated herein), comprise the entire agreement between you and publisher (and CCC) concerning this licensing transaction. In the event of any conflict between your obligations established by these terms and conditions and those established by CCC's Billing and Payment terms and conditions, these terms and conditions shall control.
14. Revocation: Elsevier or Copyright Clearance Center may deny the permissions described in this License at their sole discretion, for any reason or no reason, with a full refund payable to you. Notice of such denial will be made using the contact information provided by you. Failure to receive such notice will not alter or invalidate the denial. In no event will Elsevier or Copyright Clearance Center be responsible or liable for any costs, expenses or damage incurred by you as a result of a denial of your permission request, other than a refund of the amount(s) paid by you to Elsevier and/or Copyright Clearance Center for denied permissions.

LIMITED LICENSE

The following terms and conditions apply only to specific license types:
15. **Translation**: This permission is granted for non-exclusive world **English** rights only unless your license was granted for translation rights. If you licensed translation rights you may only translate this content into the languages you requested. A professional translator must perform all translations and reproduce the content word for word preserving the integrity of the article.
16. **Posting licensed content on any Website**: The following terms and conditions apply as follows: Licensing material from an Elsevier journal: All content posted to the web site must maintain the copyright information line on the bottom of each image; A hyper-text must be included to the Homepage of the journal from which you are licensing at http://www.sciencedirect.com/science/journal/xxxxx or the Elsevier homepage for books at http://www.elsevier.com; Central Storage: This license does not include permission for a scanned version of the material to be stored in a central repository such as that provided by Heron/XanEdu.
Licensing material from an Elsevier book: A hyper-text link must be included to the Elsevier homepage at http://www.elsevier.com . All content posted to the web site must maintain the copyright information line on the bottom of each image.

Posting licensed content on Electronic reserve: In addition to the above the following clauses are applicable: The web site must be password-protected and made available only to bona fide students registered on a relevant course. This permission is granted for 1 year only. You may obtain a new license for future website posting.
17. **For journal authors:** the following clauses are applicable in addition to the above:
Preprints:
A preprint is an author's own write-up of research results and analysis, it has not been peer-reviewed, nor has it had any other value added to it by a publisher (such as formatting, copyright, technical enhancement etc.).

Authors can share their preprints anywhere at any time. Preprints should not be added to or enhanced in any way in order to appear more like, or to substitute for, the final versions of articles however authors can update their preprints on arXiv or RePEc with their Accepted Author Manuscript (see below).
If accepted for publication, we encourage authors to link from the preprint to their formal publication via its DOI. Millions of researchers have access to the formal publications on ScienceDirect, and so links will help users to find, access, cite and use the best available version. Please note that Cell Press, The Lancet and some society-owned have different preprint policies. Information on these policies is available on the journal homepage.
Accepted Author Manuscripts: An accepted author manuscript is the manuscript of an article that has been accepted for publication and which typically includes author-incorporated changes suggested during submission, peer review and editor-author communications.
Authors can share their accepted author manuscript:

- immediately
  - via their non-commercial person homepage or blog
  - by updating a preprint in arXiv or RePEc with the accepted manuscript
  - via their research institute or institutional repository for internal institutional uses or as part of an invitation-only research collaboration work-group
  - directly by providing copies to their students or to research collaborators for their personal use
  - for private scholarly sharing as part of an invitation-only work group on commercial sites with which Elsevier has an agreement
- after the embargo period
  - via non-commercial hosting platforms such as their institutional repository
  - via commercial sites with which Elsevier has an agreement

In all cases accepted manuscripts should:

- link to the formal publication via its DOI
- bear a CC-BY-NC-ND license - this is easy to do
- if aggregated with other manuscripts, for example in a repository or other site, be shared in alignment with our hosting policy not be added to or enhanced in any way to appear more like, or to substitute for, the published journal article.

Published journal article (JPA): A published journal article (PJA) is the definitive final record of published research that appears or will appear in the journal and embodies all value-adding publishing activities including peer review co-ordination, copy-editing, formatting, (if relevant) pagination and online enrichment.
Policies for sharing publishing journal articles differ for subscription and gold open access articles:
Subscription Articles: If you are an author, please share a link to your article rather than the full-text. Millions of researchers have access to the formal publications on ScienceDirect, and so links will help your users to find, access, cite, and use the best available version.
Theses and dissertations which contain embedded PJAs as part of the formal submission can be posted publicly by the awarding institution with DOI links back to the formal publications on ScienceDirect.
If you are affiliated with a library that subscribes to ScienceDirect you have additional private sharing rights for others' research accessed under that agreement. This includes use for classroom teaching and internal training at the institution (including use in course packs and courseware programs), and inclusion of the article for grant funding purposes.
Gold Open Access Articles: May be shared according to the author-selected end-user license and should contain a CrossMark logo, the end user license, and a DOI link to the

Commercial reuse includes:

- Associating advertising with the full text of the Article
- Charging fees for document delivery or access
- Article aggregation
- Systematic distribution via e-mail lists or share buttons

Posting or linking by commercial companies for use by customers of those companies.

20. **Other Conditions**:

v1.8

SUMMARY OF CONTENTS

1.1 INTRODUCTION

Various types of evidence are commonly found in a crime scene, such as hairs, blood, and saliva. Bloodstains are important evidence that is found in violent crimes such as homicide, hit-and-run, and assaults (Jerry *et al*. 2011). In forensic science, blood is examined to provide numerous information, including an account of what has taken place (blood pattern analysis). While DNA profiling can identify the suspects and victims in the scene, blood pattern analysis can elucidate the sequence of events of the case (Liu *et al*. 2006). Additionally, determination of bloodstain age can link the bloodstain to the crime, exclude a bloodstain as being irrelevant to the crime, approximate the time since the event has occurred, and collaborate eyewitness accounts.

However, estimating the age of bloodstain is still a problem in actual forensic science practice. Although various techniques have been used to estimate the age of bloodstains (Schwarzacher 1930, Miki *et al.* 1987, Inoue *et al*. 1991, Matsuoka *et al*. 1995, Anderson *et al*. 2005, Strasser *et al*. 2007, Hanson 2010, Patterson 1960, Inoue *et al.* 1992, Andrasko 1997, Kind *et al.* 1972, Bremmer *et al*. 2010, Botonjic-Sehic *et al.* 2009, Bauer *et al*. 2003). No method has been put into routine use. The main techniques are based on spectroscopy (Schwarzacher 1930, Patterson 1960, Kind *et al*. 1972, Bremmer *et al*. 2010, Botonjic-Sehic *et al*. 2009). However, studies on the effect of substrate color and composition, humidity, and temperature on the bloodstain age estimation process are mostly lacking. Alternatively, Miki *et al.* recorded hemoglobin derivatives by measuring their electron paramagnetic resonance properties (Miki *et al.* 1987), but this approach has not been successful. Due to these errors, attempts to the techniques and decrease the error rates are constantly being made, such as by using high performance liquid chromatography (Inoue *et al.* 1991). This method is used to determine the relationship between the age of bloodstain and the ratio of hemoglobin alpha chain peak areas to the heme protein. Other techniques that have been studied are using oxygen electrode to measure the amount of oxy-

hemoglobin (HbO_2) (Matsuoka *et al*. 1995), as well as measuring the rate of RNA degradation in aging bloodstains (Anderson *et al*. 2005). In addition, near infrared (NIR) spectroscopy and atomic force microscopy (AFM) have also been used (Strasser *et al*. 2007, Jiang 2012). Nonetheless, all these methods are complex and require the use of expensive, specialized equipments, which also limits their use at crime scenes. Only the most recent age estimation technique using reflectance spectroscopy is portable and quick enough for use at the scene (Hanson 2010), but it is still limited to bloodstains found on a white background.

The simplest method for bloodstain age estimation is the observation for color change in a blood spot. The color of bloodstains changes from red to brown and can be observed with naked eyes (James 1988). This change is due to the degradation of hemoglobins. As blood leaves the body, hemoglobin saturate completely with oxygen in the ambient environment to oxy-Hb (HbO_2). Due to the lack of cytochrome *b*5 reductase, the autoxidation of HbO_2 to met-Hb form is not reversed as in *in vivo* conditions. (Smith *et al.* 2004). Patterson *et al.* utilized this property to determine the age of bloodstains by measuring the color presented (Patterson *et al.* 1960). They also found that the changes in bloodstain's reflectance spectra depend on environmental conditions such as exposure to light, temperature and humidity. It is expected that these color changes should also be detected quantitatively in a digital image of the bloodstains. Digital image analysis could be used to extract the color values of the bloodstains in different color spaces available, e.g. Red-Green-Blue (RGB) and Hue-Saturation-Value (HSV). This technique has been used to determine the relationship of the color change of peaches to storage time (Thai *et al.* 1989) and for a semi-quantitative analysis of amphetamine and methylamphetamine (Choodum 2011). Unlike the aforementioned techniques, digital image analysis requires only a digital camera and computer, both of which are readily available and thus can be easily carried out at crime scenes, making this method low-cost, simple, rapid, and truly portable.

In this study, we used digital image analysis of bloodstains to estimate the time since deposition. This method was performed under different controlled conditions, i.e. with different donors, substrate materials, humidity, light exposure, anticoagulant and temperatures to determine the effects of each factor on the age

estimation process. Moreover, the study evaluated different smartphone cameras (iPhone, iPad and Samsung Galaxy) for this purpose. Mock casework samples were also used to validate the techniques.

1.2 OBJECTIVES

This study focused on the age estimation of bloodstains by smartphone camera and digital image analysis by Image J program. The objectives are as follows:

1. To determine whether digital image analysis could be used to estimate the age of bloodstains.
2. To compare the different smartphone cameras for this purpose.
3. To evaluate whether person-to-person variations affect the color change and subsequently the age estimation process.
4. To investigate the effect of temperature, humidity, light exposure, anticoagulant and substrate materials on the age estimation of bloodstains using digital image analysis.

1.3 RESULTS AND DISCUSSION

This new method was simple, rapid, and easy to implement because the protocol only required a simple, low-cost photographic system. The system consisted of a white foam light box (2666 cm^2 inner surface area) illuminated evenly with a Sylvania Osram DULUX S 9-Watt Cool White bulb (G32-2 pin base, 600 lumens, 4100K color temperature, Sylvania Osram, Thailand) (Figure1) Color analysis was carried out using an Image J macro – a simple script that extracts color values from the digital photos taken with a smartphone camera. The color values were easily quantifiable and indicated that bloodstains color change with time. Many factors affected the color values, including smartphone camera, temperature, humidity, light exposure, the addition of anticoagulant, and substrate color.

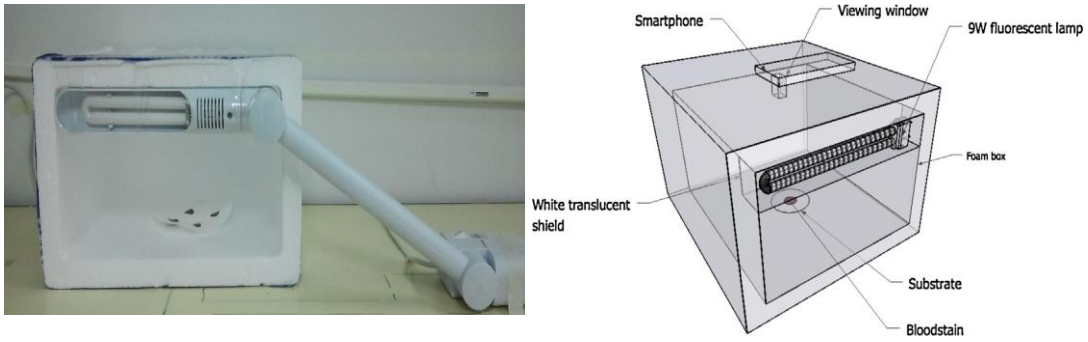

Figure 1: A is home-made light box made from a foam box and a desk lamp and B is a 3D sketch of the photographic system used in this study.

1.3.1 Color value selection

The first experiment was done to determine whether the color changes with age for bloodstains and also which color changes the most. Blood samples were collected from four volunteers, three females and one male. 50 microliters of blood were dropped onto filter paper. A total of five bloodstains were used for each person. Three smartphone cameras (iPhone 4, iPad 2 and Samsung Galaxy S Plus) were used to capture digital images at 15 minutes, 30 minutes, 1 hour, 3 hours, 6 hour, 12 hours, 24 hours, then once a day until 7 days and every week until 1.5 month or approximately 42 days. All settings of smartphone cameras were set to automatic (white balance, ISO, focusing mode, and metering mode). The smartphone was placed on the top of a light box that was created to control the amount of light (Figure 1). Five photographs were taken for each bloodstain. All digital images are formed from three 8-bit channels: red, green and blue color. The values of RGB range from 0 to 255. RGB can be converted to other color spaces such as cyan, magenta, yellow and key (CMYK) and hue, saturation, lightness (HSL). Color extraction and conversion was performed automatically using an in-house Image J (http://imagej.nih.gov) macro – a computer script – to automate the batch processing (Appendix 1).This enabled many photographs and stains to be analyzed concurrently. The output comma-separated-values (CSV) file was imported into Microsoft Excel and R statistical program for further analysis.

Each color value from the three color spaces (RGB, CMYK, and HSL) was linearly regressed to time since deposition. The correlation coefficient of each relationship was then determined. The statistical linear model has a correlation coefficient bound 0 and 1.0 (https://en.wikipedia.org/ wiki/Correlation_coefficient) Highly correlated factors have their correlation coefficients close to 1.0. This process was done to determine the best predictor for time since deposition. As expected, collection time was transformed using base-10 logarithm to linearize the relationship between color values and time (in hours) and the biphasic change of hemoglobin derivatives build on fitted a local polynomial regression (LOESS). The color values varied in their correlation with time since deposition. M (magenta) and S (saturation) correlated highly with time since deposition with R^2 values of 0.966 and 0.911 (Table 1) using linear modeling. Thus, magenta was selected for further studies due to its high correlation with time since deposition. The decrease in these color values followed a logarithm decay pattern – rapid decrease in the beginning followed by a slow decrease at later time-points (Figure 3). The first two time-point (15 and 30 min) and the time-points over 6 weeks were excluded from the linear models, as the decrease in color values in the first hour was even more rapid than a logarithmic function. The underlying phenomenon has been explained by Bremmer *et al* (Bremmer *et al.* 2010). In the earliest stages when blood leaves the body, oxyhemoglobin rapidly degrades to methemoglobin and hemichrome. The color of the bloodstains is determined by the ratio of three hemoglobin derivatives (oxy-hemoglobin, met-hemoglobin, and hemichrome) in the bloodstain, since each derivative has a unique absorption spectrum. The fraction of each hemoglobin derivative changes with time (James *et al.* 1988, Chen and Ikeda-Saito *et al*. 2008, Marrone and Ballantyne 2009). The results of our experiment indicate that the color change due to this denaturation process was quantifiable using a digital image analysis. The change in color of blood from bright red to brown can be summarize in RGB terms as follows: the difference between red (255,0,0) and brown (150,75,0) is the decrease in R channel and increase in G channel.

Table 1: The correlation coefficient of each color value and time since deposition in a regression model

Parameter	Calibration equation	R^2
R and log time	y = -6.0x+81.6	0.349
G and log time	y = 6.48x+25.6	0.726
B and log time	y = 3.78x+25.6	0.434
C and log time	y = 0x+0	0.000
M and log time	y = -0.119x + 0.688	0.966
Y and log time	y = -0.0843x+0.696	0.896
K and log time	y = 0.0235x+0.680	0.349
H and log time	y = -41.1x+98.9	0.224
S and log time	y = -0.0843x+0.531	0.911
L and log time	y = -0.00392x+0.209	0.026

1.1.2 Smartphone camera comparison

The bloodstains on filter paper kept in the dark at 25^{o}C were photographed with three different smartphone cameras (iPhone 4s, iPad 2 and Samsung Galaxy S Plus). The five pictures at each time-point from each camera were analyzed. The Samsung Galaxy S Plus was the most suitable camera for bloodstain age estimation, as it displayed the narrowest 95% confidence interval for magenta values (Figure 2), meaning that the predictions using a model based on the Galaxy S Plus would be the most precise. The confidence interval is the interval in which the true mean would fall in 95% of time. The size of the interval depends on the spread of the raw data. As such a narrow interval means that there were less variations in the pictures taken with the Samsung. (http://www.stvc.ac.th/elearning/stat/csu5.html)

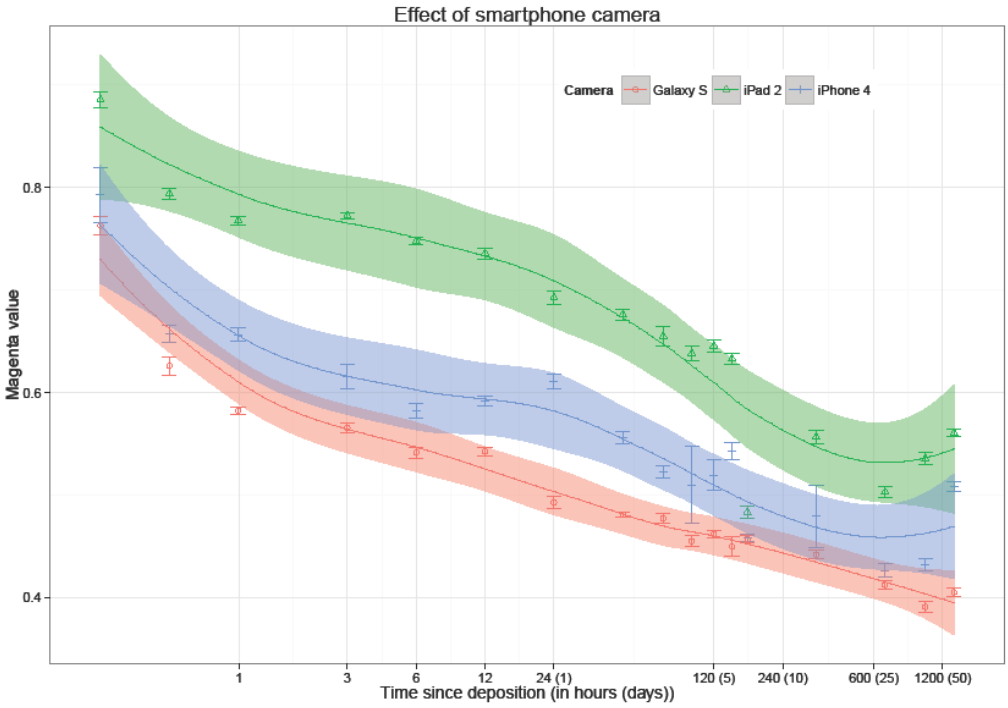

Figure 2: Average and 95% confidence interval of magenta values obtained from bloodstains (*N*= 5 for each smartphone) using three smartphone cameras (red is Galaxy S, green is iPad 2, and blue is iPhone 4)

In the earliest stages, the magenta values of three cameras were different, possibly due to the differences in both hardware (e.g. sensors type and size) and software (image processing). The specification of camera smartphone in each brand is shown in Table 2. (http://www.techxcite.com/topic/10984.html; http://www.techmoblog.com/ipad-4-vs-ipad-3-vs-ipad-2-spec-comparison/; http://www.thaimobilecenter.com/spec/Samsung_ Galaxy_S_Plus_i9001.asp)

Table 2: The specification of various smartphone cameras

Smartphone	iPhone 4s	iPad 2	Samsung Galaxy Plus
Pixel density	3264×2448	1024×768	2592×1944
Focus	autofocus	-	autofocus
Flash	LED flash	no flash	flash

The Apple iPad 2 and iPhone 4s cameras displayed fluctuating magenta values with increasing time, while the magenta values obtained from the Samsung Galaxy S Plus consistently decreased with time. Using linear models, Samsung Galaxy S Plus had the highest a correlation coefficient (0.935), followed by iPhone 4s (0.796), and iPad 2 (0.637).

Although, the iPhone's back-illuminated sensor technology allows more light to hit the sensor by repositioning the wiring (Choodum 2011), the improved sensitivity to light did not improve the results obtained when compared to the smaller, older image sensor in the Galaxy S Plus camera. This could be due to the evenly lit and bright light box (Figure 1) as well as the software-based color correlation algorithms. The bright conditions must have negated the need for a bigger sensor. While humans see the same color from object under different lights, digital cameras cannot do so and relies on these algorithms to correct for the differences (Jiang *et al.* 2012). Unlike the RAW format from digital single-lens reflex (DSLR) camera, a compressed JPEG file from smartphone cameras has undergone image processing, including color correction. A DSLR was not used for this study, as similar studies comparing smartphone cameras and DSLRs did not find any difference between the two categories or even showed that smartphone cameras had higher sensitivity and less relative errors than DSLRs for these forensic purposes (Choodum 2011). Our results suggest that the three smartphones used different algorithms for color balancing, as pictures of the same bloodstains gave different color value. The goal of a smartphone camera is to produce a good-looking image with the least user

effort required. Apple Inc., the maker of iPad 2 and iPhone 4s, has patents pertaining to image processing related to color correction and these could have affected the color values of the bloodstains.

1.1.3 Within and between-person variation

Blood samples were collected from four volunteers to assess person-to-person variation. The volunteers are three females and one male. All were Asian, healthy and non-smoker. Five bloodstains from each person were dropped onto filter paper and kept in a dark room at 25^{o}C. The data were collected at 15 minutes, 30 minutes, 1 hour, 3 hours, 6 hours, 12 hours, 24 hours, then once a day until 7 days and every week until 42 days. All bloodstains were then analyzed using Samsung Galaxy S Plus. Figure 3 shows the between-person variation with passing time. The main trend observed is the biphasic decrease in magenta value. Only minimal variations were observed within-person, as indicated by the clustering of the magenta values from the five bloodstains of each donor. As for between-person variation, the overlap in the confidence interval of each donor's LOESS fit suggests that there was no person-to-person variation. Previous studies showed similar results with the findings in this study. Anderson *et al.* found an ANOVA value of 0.93 for the ratio (18S: β-actin). Also, for bloodstain age estimation using reflectance spectroscopy, no significant person-to-person variation was found among 40 bloodstains from eight donors (Patterson, 1960). The lack of variation could be explained by the similarity in the amount of hemoglobins, as the volunteers were from the same age group and healthy (https://sites.google.com/site/bodybalanceu/med-leuxd-laea-swn-prakxb-khxng-med-leuxd). In summary, the age estimation of bloodstain with digital image analysis has no significant within-person and between-person variations. As such, it could be an appropriate technique to estimate bloodstains age.

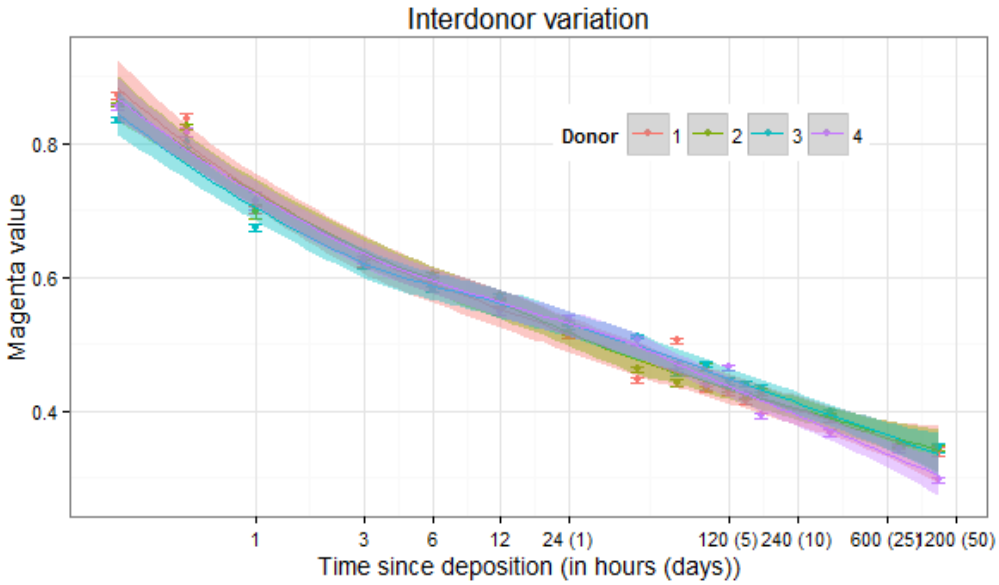

Figure 3: The change in magenta value of each donor (N=4) (red is the first person, green is the second, blue is the third and purple is the fourth) and 95% confidence intervals of magenta values obtained from five bloodstains of each donor

1.1.4 Age estimation of bloodstains

We used the data from the person-to-person variation study to assess prediction accuracy for unknown stains. Bloodstains were divided into two subsets (training set and validation set), according to a standard statistical approach called one round cross-validation (Bremmer *et al.* 2010). The data from training set (70 percentages of all data) and validation set (30 percentages of all data) were used to create simple linear regression model. The age of blood up to 42 days was estimated. A simple age estimation method using linear regression with magenta value (m) as the predictor for time since deposition in hours (t):

$$t = \frac{m - 0.688}{-0.119}$$

In this study, we observed better accuracy for younger bloodstains than older bloodstains, which can be explained because hemoglobin denatures faster in the beginning of the aging process (Bremmer *et al.* 2011) (Figure 4). The simple prediction model using only magenta values tended to underestimate the actual age of bloodstains. Most points shown after 10 days fall below the line of unity.

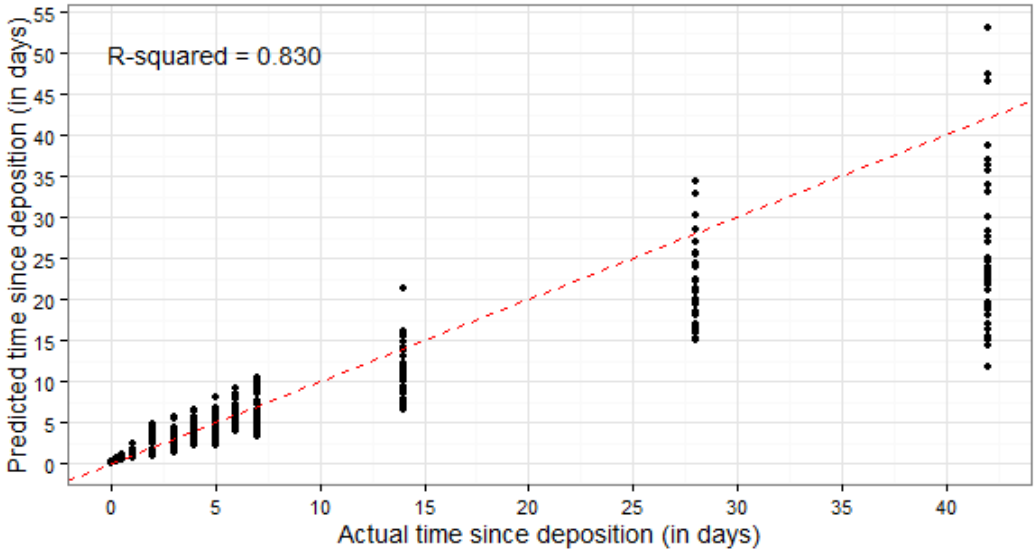

Figure 4: Predicted age of bloodstains versus the actual age. Means are shown as black dots. The line of unity is plotted as a dashed red line. The adjusted R- squared of the relationship was 0.830.

As such, the range of predicted time since deposition increased with the bloodstain age, which is a disadvantage that must be kept in mind in real forensic casework. In other words, these results demonstrate that image analysis is suitable for short term age estimation. A similar result was reported by Edelman *et al.* who used hyperspectral imaging to estimate the age of bloodstains. However, Edelman *et al.*'s method is more difficult and complex than the one proposed here, as a specialized instrument is needed for the estimation process. However, before the image analysis for age estimation of bloodstains can be applied in practice, other key factors that affect the degradation process of hemoglobin must be investigated. These factors include, but are not limited to, temperature, humidity and light exposure. If the effect size of these factors could be quantified, a smartphone application could ever create to estimate bloodstain age in a crime scene.

1.1.5 Environmental effects on the aging process

1.1.5.1 Temperature

The effect of temperature on digital image analysis technique was investigated. Five bloodstains on filter paper stored in dark room at -20°C, 4°C and 25°C. The data were collected at 15 minutes, 30 minutes, 1 hour, 3 hours, 6 hours, 12 hours, 24 hours, then once a day until 7 days and every week until 42 days. All data were plotted for each temperature as a function of average of magenta value with time since deposition and a 95% confidence interval was calculated for each temperature.

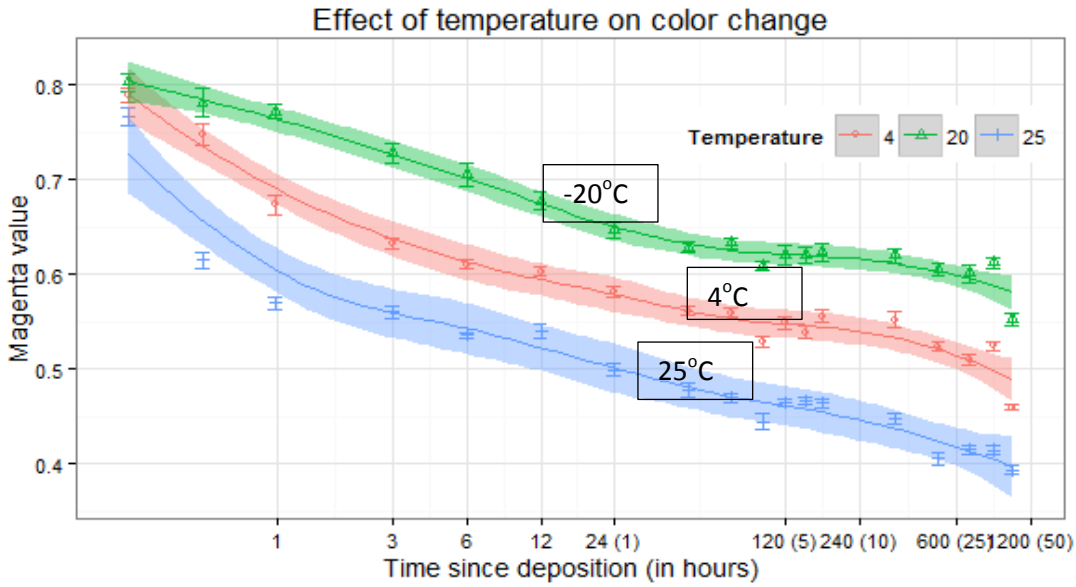

Figure 5: Average and 95% confidence intervals of magenta values obtained from bloodstains (*N*= 5 for each humidity level) kept at-20°C (green), 4°C (red) and 25°C blue). Higher temperature increased the rate of hemoglobin denaturation.

The initial (0 hour), magenta values were very similar in all temperatures. The difference in magenta value became more obvious at 15 minute, when the first measurements were taken. The slopes of three temperature levels were different, i.e. the rate of change, or slope, of the magenta values increased with increasing temperature. The slope of bloodstains at -20°C was smallest and at 25°C was largest. After three hours, the rate of change for all three temperature levels were constant, as evidenced by the parallel lines seen in Figure 5. From this data, it can be

concluded that high temperatures sped up the auto-oxidation of oxyhemoglobin to met-hemoglobin and hemichrome. After 40 days, the data of all temperature levels fluctuated. This time-point seemed to be the limit of bloodstain age that can be analyzed by the technique proposed in this study. The analysis of the effect of temperature was imperative to the bloodstain age estimation process, as the bloodstains in an actual crime scene will also be affected by the ambient temperature at the scene. Knowing the effect of temperature can help a forensic investigator obtain a better estimate of the time since deposition. In Thailand the average temperature is $27.2 \pm 1.6^{o}C$ and there is almost no change between each season which is different form the other country. The variation of temperature affect to the changing the oxidize rate of hemoglobin.

1.1.5.2 Humidity

Five bloodstains on filter paper and stored at three humidity levels were compared: 30%, 50% and 80% relative humidity. The data were collected at 15 minutes, 30 minutes, 1 hour, 3 hours, 6 hours, 12 hours, 24 hours, then once a day until 7 days and every week until 42 days. Average magenta values were plotted against time since deposition and result is shown in Figure 6. The difference in magenta values were clear since the first measurements.

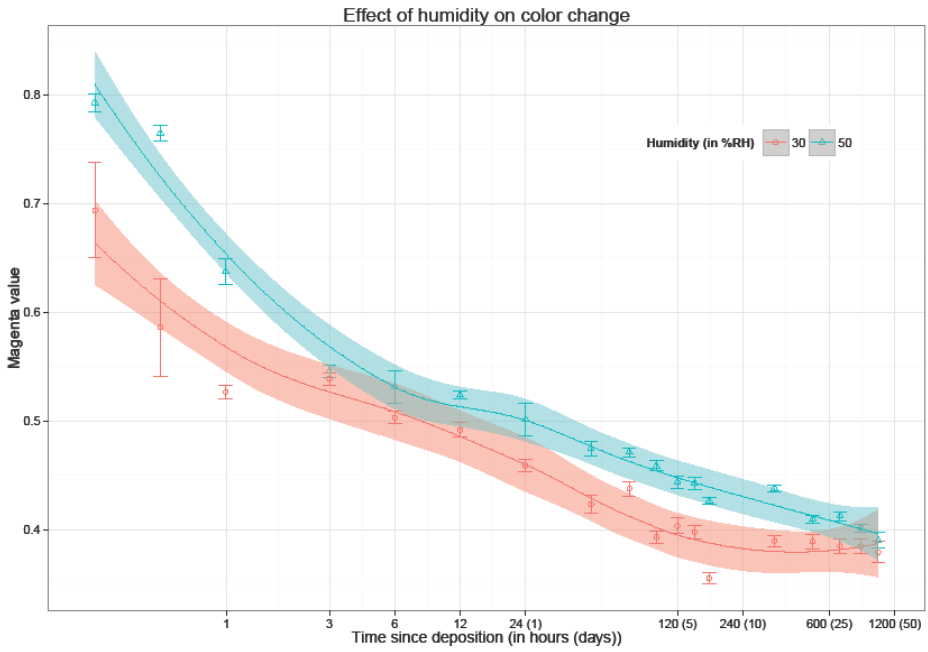

Figure 6: Average and 95% confidence intervals of magenta values obtained from bloodstains (*N* =5 for each humidity level) kept at 30% (red) and 50% (blue) relative humidity at 25%^{O}C. Higher humidity slowed the color change process

With increasing time, the magenta value of bloodstains kept at 30% RH decreased faster than the bloodstains at 50% RH. This result is consistent with the study of Bremmer *et al.* (Bremmer *et al.* 2011), who reported about the rate of the change from met-hemoglobin to hemichrome: high humidity sped up oxidation more than low humidity. Over the course of two months that the color change was monitored, it was found that magenta values of both humidity levels were fluctuating, which could be because the camera of smartphone found it difficult to focus on old stains. Also, humidity level was controlled using an in-house humidity chamber constructed from a foam box, computer fans, and silica gels. As such, the humidity level could have fluctuated in between the scheduled silica gel replacements. Bloodstains kept at 80% RH could not be investigated due to excessive fungal growth on the stains.

1.1.5.3 Light exposure

Five bloodstains on filter paper were kept in the dark, under fluorescent lighting, and under natural sunlight. The data were collected at 15 minutes, 30 minutes, 1 hour, 3 hours, 6 hours, 12 hours, 24 hours, then once a day until 7 days and every week until 42 days. The averages of magenta values were plotted with time since deposition. The results indicate that exposure to sunlight produced a different color change pattern when compared with bloodstains kept in the dark and under fluorescent light (Figure 7). At 15 min, almost no difference in magenta values were observed between the different conditions. After 30 min, bloodstains exposed to sunlight had significantly lower magenta values than bloodstains kept in the dark and exposed to fluorescent light. After one hour, bloodstains kept in the dark and under fluorescent light were still indistinguishable. The samples exposed to sunlight had their colors changed faster in the early hours (larger drop in magenta value). It was suspected that sunlight accelerated the rate of change from oxy-hemoglobin to met-hemoglobin and from met-hemoglobin to hemichrome due to two reasons. One, sunlight increased the temperature of the bloodstains. The previous experiment with temperature showed that temperature has a positive correlation with the rate of color change. Two, light could have sped up the rate of oxidization of hemoglobin (Bremmer *et al.* 2011).

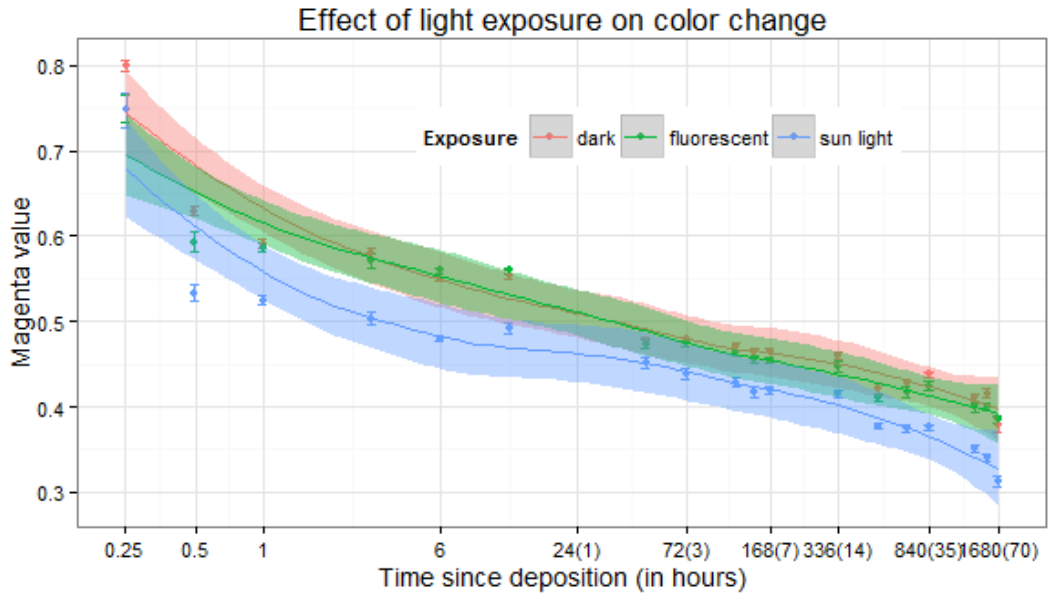

Figure 7: Average and 95% confidence intervals of magenta values obtained from bloodstains (*N* =5 for each humidity level) kept in the dark (red), under fluorescent lighting (green), and under natural sunlight (blue). No difference was observed for the bloodstains in the dark and under fluorescent light.

1.1.5.4 Anticoagulant

This experiment compared the change in color of blood with and without added anticoagulant. Two anticoagulants used to study: EDTA and heparin. All bloodstains were kept at 25^{o}C and the data collected at 15 minutes, 30 minutes, 1 hour, 3 hours, 6 hours, 12 hours, 24 hours, then once a day until 7 days and every week until 42 days. The averages of magenta value were plotted with time since deposition. The result of the effect of anticoagulant is shown in Figure 8.

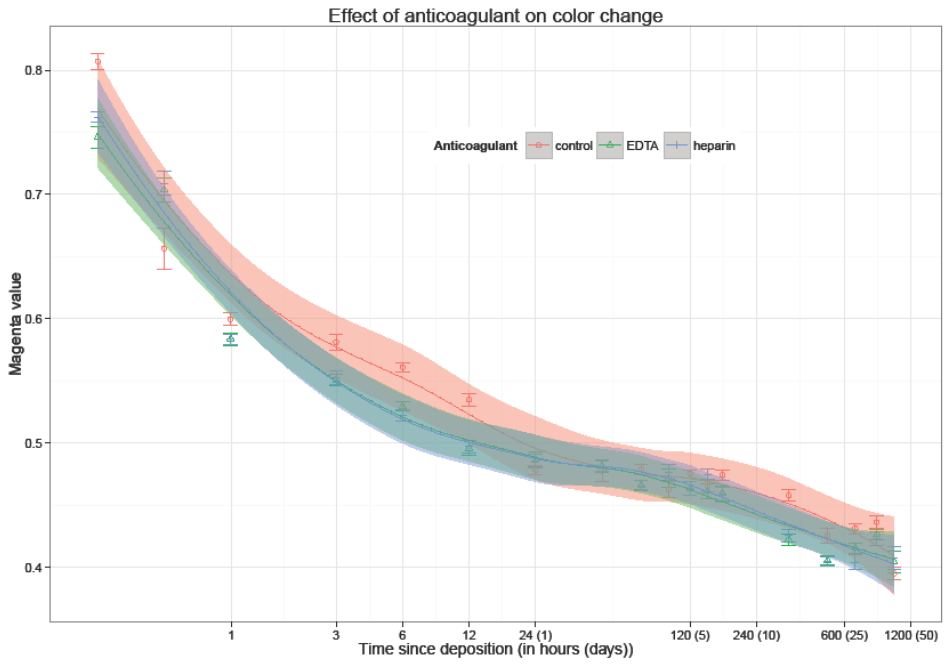

Figure 8: Average and 95% confidence interval of magenta values obtained from control bloodstains (red), bloodstains mixed with EDTA (green) and bloodstains mixed with heparin (blue).

Both EDTA and heparin did not affect the magenta value of bloodstains, as shown by the overlapping 95% confidence intervals between control bloodstains and stains mixed with anticoagulants. From Figure 8, only at two time-points (30 minutes and one hour) were slight differences observed. One previous study that investigated anti-coagulant effect on bloodstain color also did not find any influence of anticoagulant on the aging process of bloodstains (Bremmer *et al.* 2010). In general, anticoagulant changes red blood cells shape to spherical. Thus, it was concluded that anti-coagulant did not affect the method for bloodstain age estimation used in this study (http://www.microscopy.ahs.chula.ac.th/newmicros/ lecture/bloodcollecting.pdf).

1.1.6 The effect of substrate

In the crime scene, we are not able to control the position of bloodstains and type of substrate that the blood is found on. As the method proposed depends on bloodstain color, substrate color might interfere with the measurement

process. The study of the effect of substrate is therefore necessary. Five bloodstains dropped onto various substrates including cotton, denim, filter paper, glass, leather and wall. All bloodstains were stored in dark at 25^{o}C. The data were collected at 15 minutes, 30 minutes, 1 hour, 3 hours, 6 hours, 12 hours, 24 hours, then once a day until 7 days and every week until 42 days. The averages of magenta value were plotted with time since deposition. In Figure 9, two substrates (filter paper and cotton) showed possibility of allowing prediction of the age of bloodstain. Both substrates were light color. Although glass, wall (gypsum) and leather were light color like the filter paper and cotton, they reflect more light. Thus, the average magenta values obtained were highly variable. The slightly rough surfaces spaced with troughs of the gypsum and leather also negatively impacted the measurement of magenta values. Also, it was not possible to obtain enough variations in color from bloodstains on denim. In summary, the characteristics of substrate affected the process of measuring bloodstain color and subsequently the prediction of age estimation of bloodstains by using digital image analysis. The extraction of bloodstains from substrate, as carried out by Hanson and Ballantyne (Hanson *et al*. 2010), could be useful for the proposed method.

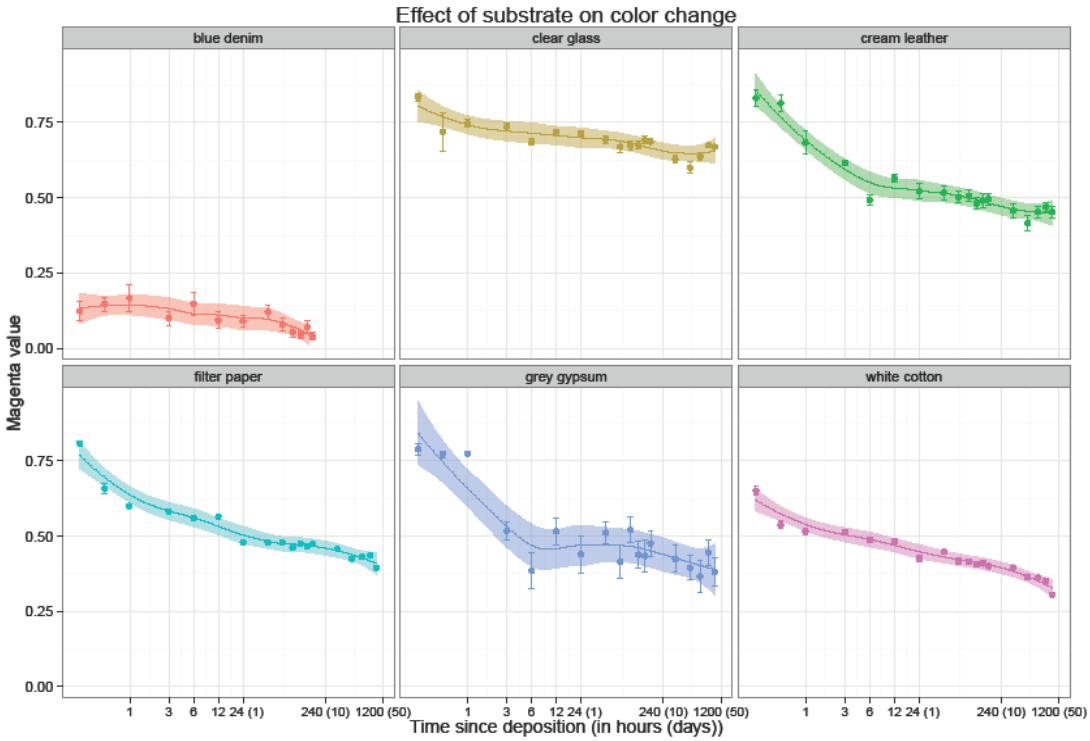

Figure 9: Average and 95% confidence intervals of magenta values from bloodstains deposited onto six substrates (blue denim is red line, clear class is brown, leather is green, paper is light blue, gypsum is blue and white cotton is purple)

1.1.7 Mock case work

Our technique was highly accurate under controlled conditions. In real life, one is not able to control the substrate that the blood will fall on nor the environment of the crime scene. The study of mock case work was used to validate the technique proposed in this study. A number of bloodstains were deposited on various substrates: cream leather, cloth, denim, brown flagstone, shiny paper, plastic dish, shoes and stainless steel. These items had been scattered in a room to simulate a typical apartment. Environmental effects such as temperature, light and humidity was not controlled for (Appendix B). The data was collected at 15 minutes, 30 minutes 1 hour, 3 hours, 6 hours, 12 hours, 24 hours, and then once a day until 7 days and every week 42 days. The result showed that the magenta value fluctuated in all substrates except the bloodstains on cloth (Figure 10 and 11), where the pattern in the data

suggested that it should be possible to estimate bloodstain age for up to the last day that the measurement was taken (42 days). The reason for the low variability between the stains at different time points for cloth was (1) probably the white background of the cloth and (2) the cloth was not exposed directly to sunlight.

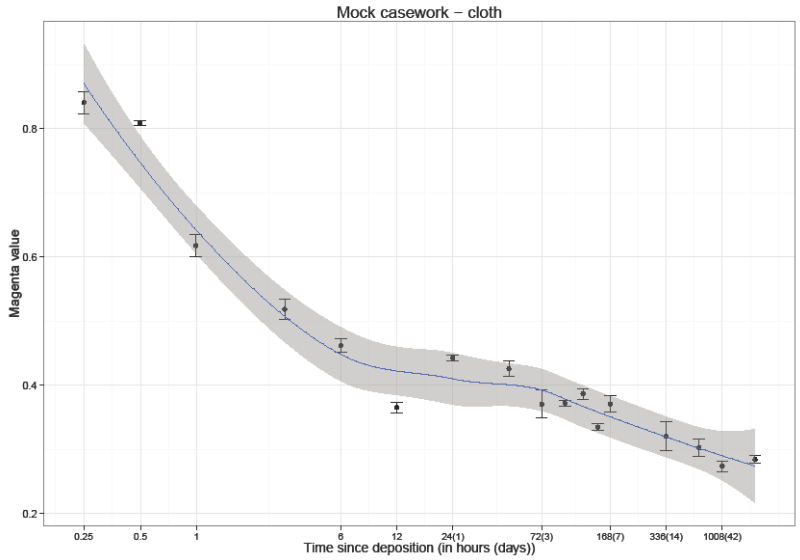

Figure 10: Average and 95% confidence intervals of magenta values from bloodstains deposited onto white cloth

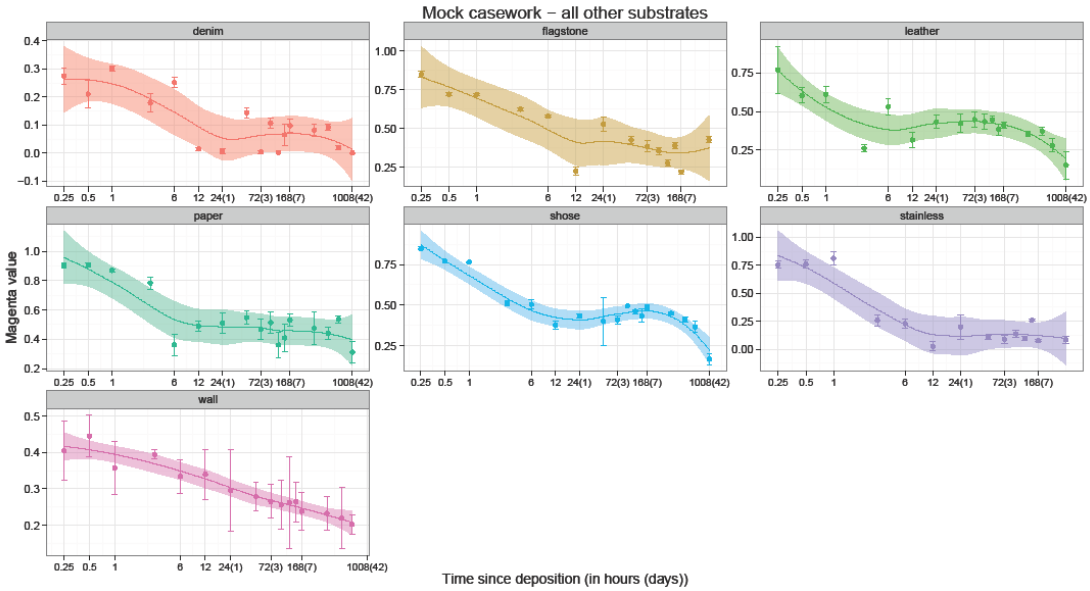

Figure 11: Average and 95% confidence intervals of magenta values from bloodstains deposited onto various substrate in mock work

The other substrates (Figure 11) had no detectable pattern that could be used to estimate the bloodstain age. This fluctuation was observed as early as 30 minutes. The variations in the M values differed with each substrate. It was believed that the substrate characteristics, particularly the color of the substrates themselves, interfered with the color values that were obtained. For example, it was more difficult to quantify the change in bloodstain color when the substrates were dark color like denim. The non-porous nature of stainless steel resulted in clumping of the bloodstains and uneven distribution of bloodstain thickness and color. As the different substrates were differently exposed to temperature and humidity (e.g. substrates that were located closer to the bathroom were probably exposed to higher humidity and vice versa). The environment can speed up or slow down the denaturation process such as oxidation of hemoglobin. Further improvements are needed before this method is applicable to casework samples.

1.4 Concluding remarks

Bloodstains are commonly found in crime scenes, especially in violent crimes. Being able to predict bloodstain age can aid investigation, for example, predicting the time of incident in which there is no witness. Many techniques are employed for said purpose and it is still an active area of research. However, most studies require complex, dedicated instruments and are expensive. Currently there is no method that shows high accuracy of prediction and that has been applied in forensic case work.

This study is a new method to predicted age of bloodstains in the crime scene that is easy and cheap. We can use digital image analysis to study the change in color in bloodstains caused by the different ratios of hemoglobin derivatives. Our result of demonstrated the smartphone brand, temperature, humidity and light exposure affected the color change process. The brand of smartphone affect the color values that were extracted. The environment cam speed up or slow down the denaturation process such as oxidation of hemoglobin. This information is necessary to select a model or create a model for prediction of age of bloodstain in the future. The active developer communities of both Google’s Android OS have the potential to

develop a real-time application and we envision a smartphone that could give more accurate for prediction of age of bloodstain. Moreover, the smartphone camera is compact and convenient for using in a crime scene.

This technique has high accuracy and precision in controlled conditions and can accurately predict bloodstain age of less than 10 days. Similar to previously used spectroscopy-based technique, our developed method works well white or light-colored substrates. However, with dark-colored substrates, the background color interferes with the color analysis. In the future, one might solve this problem by extracting the bloodstains from the substrate. In an actual crime scene, it is impossible to dictate the environmental conditions and thus our developed prediction equation might be too simplistic. Incorporating relevant parameters could extend the usability of the method to real casework.

REFERENCE

Andrasko, J. (1997). The estimation of the age of bloodstains by HPLC analysis. J. Forensic Sci. 42: 7.

Anderson, S., B. Howard, et al. (2005). A method for determining the age of a bloodstain. Forensic Sci. Int. 148: 37-45.

Bauer, M., S. Polzin, et al. (2003). Quantification of RNA degradation by semiquantitative duplex and competitive RT-PCR: a possible indicator of the age of bloodstains?. J. ForensicSci. Int. 138: 94-103.

Botonjic-Sehic, E., C. W. Brown, et al. (2009). Forensic application of near-infrared spectroscopy: aging of bloodstains. Spectroscopy. 24: 42-48.

Bremmer, R. H., A. Nadort, et al. (2010). Age estimation of blood stains by hemoglobin derivative determination using reflection spectroscopy. J. Forensic Sci. Int. 206(1-3): 166-171.

Chen, H., M. Ikeda-Saito, et al. (2008). Nature of the Fe–O-2 bonding in oxy-myoglobin: effect of the protein. J. Am. Chem. Soc. 130: 14778-14790.

Choodum, A. and N. N. Daeid (2011). Digital image-based colourimetric [corrected] tests for amphetamine and methylamphetamine. Drug Test Anal 3 (5): 277-282.

Hanson, E. K. and J. Ballantyne. (2010). A Blue spectral Shift of Hemoglobin Soret band Correlates with the Age (Time Since Deposition of Dried Bloodstains. PLoSONE. 5(9).

Inoue, H., F. Takabe, et al. (1992). A new marker for estimation of bloodstain age by high performance liquid chromatography. Forensic Sci. Int. 57: 17-27.

Inoue, H., F. Takabe, et al. (1991). Identification of fetal hemoglobin and simultaneous estimation of bloodstain age by high-performance liquid chromatography. Int. J. Legal Med. 104: 127-131.

Jain, A. K. (1989). Fundamental of digital image processing. NT: Prentice-Hall.

James, S. H. (1988) Interpretation of bloodstains evidence at crime scences. in:CRC series in Practical Aspects of Criminal and Forensic Investigations.

Jerry Chisum, W. and E. Turvey (2011). Reconstruction using bloodstain evidence. 225 Wyman Street, Waltham, MA 02451, USA, Academic Press is an imprint of Elsevier: 231-240.

Jiang. J, Y. Zhao, S-g. Wang, Color correction of Smartphone Photos with Prior Knowledge. Imaging and Printing in a Web 20 World III, SPIE Proceedings, Burlingame. CA, USA, 2012.

Kind, S. S., D. Patterson, et al. (1972). Estimation of the age of dried blood stains by spectrophotometric method. J. Forensic Sci. 1: 27-54.

Liu YZ. Xiao, P. Guo YF, Xiong DH, Zhao l.J, et al. (2006). Genetic linkage of human height is confirmed to 9q22 and Xq24. Hum genet 119: 295-304.

Marrone, A. and J. Ballantyne (2009). Changes in dry state hemoglobin over time do not increase the potential for oxidative DNA damage in dried blood. PLoSONE. 4: 5110.

Miki, T., A. Kai, et al. (1987). Electron spin resonance of bloodstains and its application to the estimation of time after bleeding. Forensic Sci. Int.35: 149-158.

Matsuoka, T., T. Taguchi, et al. (1995).Estimation of bloodstain age by rapid determinations of oxyhemoglobin by use of oxygen-electrode and total hemoglobin. Biol. Pharm. Bull 18: 1031-1035.

Patterson, D. (1960). Use of reflectance measurements in assessing the colour changes of ageing bloodstains. Nature. 187: 688-689.

Rauschke, J. (1951). Beitragezurfrage der alterbestimmung von blutspuren. Int.J.Legal Med. 40: 578-584.

R.H. Bremmer, G. Edelman, T.D. Vegter, T. Bijvoets, M.C.G. Aalders, Remote spectroscopic identification of bloodstains, Journal of Forensic Sciences 56 (2011) 1471-1475.

R.H. Bremmer, D.M. de Bruin, M. de Joode, W.J. Buma, T.G. van Leeuwen, M.C. Aalders, Biphasic oxidation of oxy-hemoglobin in bloodstains, PLoS ONE 6 (7) (2011) e21845.

Scheller, H., Dtsch, et al. (1937). UntersuchungenzurBrauchbarkeit der Sanguicit-und KaufmannschenBenzidin-Methylalkoholprobe fur den forensischen Blutnachweis. Med. 28: 217.

Schwarzacher. (1930). Determination of the age of bloodstains. Am. J. Police Sci.1.

Smith, A. (2004). Basic Medical Biochemistry. L. W. Wilkins.

Strasser, S., A. Zink, et al. (2007). Age determination of blood spots in forensic medicine by force spectroscopy. Forensic Sci. Int. 170: 8-14.

Thai, Shewfelt, et al. (1989). The color change of peaches storage Food Research International. 36: 669-676.

Wittenberg, J. B., B. A. Wittenberg, et al. (1970). On the state of the iron and the nature of the ligand in oxyhemoglobin. Proc.Natl.Acad.Sci. U.S.A. 67: 1846-1853.

https://en.wikipedia.org/wiki/Correlation_coefficient 25/11/2015

https://sites.google.com/site/bodybalanceu/med-leuxd-laea-swn-prakxb-khxng-med-leuxd 06/11/2015

http://www.microscopy.ahs.chula.ac.th/newmicros/lecture/bloodcollecting.pdf 09/11/2015

http://www.stvc.ac.th/elearning/stat/csu5.html 25/11/2015

http://www.techxcite.com/topic/10984.html 25/11/2015

http://www.techmoblog.com/ipad-4-vs-ipad-3-vs-ipad-2-spec-comparison/ 25/11/2015

http://www.thaimobilecenter.com/spec/Samsung_Galaxy_S_Plus_i9001.asp 25/11/2015

Appendix A

The macro command is a simple script that extracts color values from the digital photos taken with a smartphone camera. It was used for color analysis which carried out using the ImageJ program. Multiple images can be analyzed with only a few mouse clicks, which is an advantage of the method. The work flow of the macro from start to finish is shown in the following diagram

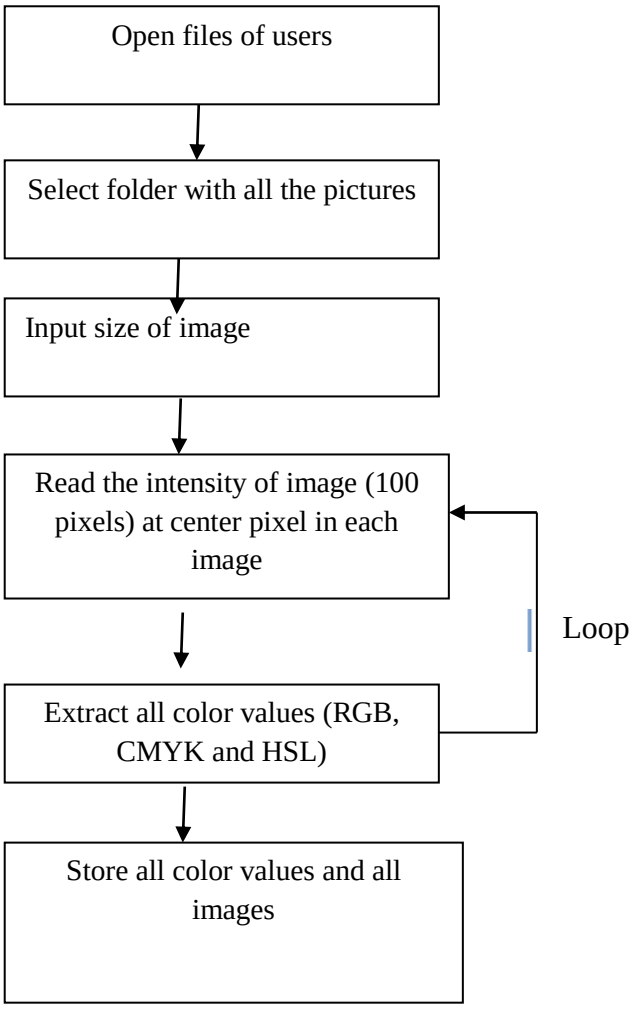

batch RGB analysis

```
//extract surface area and ndvi over the whole plot for trees and grasses

//run("Memory & Threads...", "maximum=1600 parallel=8 run");

dir2 = getDirectory("Choose Source Directory "); //prompt user for destination
directory

dir3 = getDirectory("Choose Results Directory "); //promt user for destination
directory for results file

list2 = getFileList(dir2); //get a list of the files

setBatchMode(true);

//define two new functions to get max and min from 3 values
function minOf3(n1, n2, n3) {
returnminOf(minOf(n1, n2), n3);
}

function maxOf3(n1, n2, n3) {
returnmaxOf(maxOf(n1, n2), n3);
}


//reset previous runs
run("Clear Results");
row=0;

//Prompt user for the image size and find the midpoint pixel
w = getNumber("Enter image width (x) ", 1);
h = getNumber("Enter image height (y) ", 1);
```

```
w = w/2;
h = h/2;

//Loop through the images in the folder and extract interested values
for (z=0; z<list2.length; z++) {
open(dir2+list2[z]);        //opens every image
showProgress(z+1, list2.length);

        start = getTime();        // Get current time for progress bar

//calculate RGB

        v = getPixel(w, h);
        r = (v & 0xff0000)>>16;
        g = (v & 0x00ff00)>>8;
        b = (v & 0x0000ff);
        setResult("R", row, r);
        setResult("G", row, g);
        setResult("B", row, b);

//calculate CMYK

        c = 1.0 - r/255;
        m = 1.0 - g/255;
        y = 1.0 - b/255;
        k = minOf3( c, m, y);
        if ( k == 1.0 ) {
                c = m = y = 0;
                }
        else {
                s=1.0 - k;
                c = ( c - k ) / s;
```

```
            m = ( m - k ) / s;
            y = ( y - k ) / s;
        }

        setResult("C", row, c);
        setResult("M", row, m);
        setResult("Y", row, y);
        setResult("K", row, k);

//calculate HSV and HSL

        rScale = r/255;
        gScale = g/255;
        bScale = b/255;

        M = maxOf3(rScale, gScale, bScale);
        m = minOf3(rScale, gScale, bScale);

        r = (M - rScale) / (M - m);
        g = (M - gScale) / (M - m);
        b = (M - bScale) / (M - m);
        V = maxOf3(rScale, gScale, bScale);
        L = ( M + m) / 2;

        if ( M == 0 ) {
            S = 0;
            S2 = 0;
            H = 180;
        }
        else {
            S = (M - m) / V;
            S2 = (M - m) / (1 - abs(2*L - 1));
```

```
		}

		if ( rScale == M ) {
			H = 60*(b-g);
		}
		if ( gScale == M ) {
			H = 60*(2+r-b);
		}
		if ( bScale == M ) {
			H = 60*(4+g-r);
		}
		if ( H>= 360 ) {
			H = H - 360;
		}
		if ( H< 0 ) {
			H = H + 360;
		}
		setResult("H", row, H);
		setResult("S", row, S);
		setResult("V", row, V);
		setResult("S2", row, S2);
		setResult("L", row, L);

		row++;  //increment the row for each image

		//updateResults();
saveAs("Results", dir3+"imageData.txt");
```

2. Batch RGB for random point

```
//extract surface area and ndvi over the whole plot for trees and grasses

//run("Memory & Threads...", "maximum=1600 parallel=8 run");

dir2 = getDirectory("Choose Source Directory "); //prompt user for destination
directory

dir3 = getDirectory("Choose Results Directory "); //promt user for destination
directory for results file

list2 = getFileList(dir2); //get a list of the files
subloop=0;
pic=1;
setBatchMode(true);

//define two new functions to get max and min from 3 values
function minOf3(n1, n2, n3) {
returnminOf(minOf(n1, n2), n3);
}

function maxOf3(n1, n2, n3) {
returnmaxOf(maxOf(n1, n2), n3);
}

//reset previous runs
run("Clear Results");
row=0;

//Prompt user for the image size and find the midpoint pixel
w = getNumber("Enter image width (x) ", 640);
h = getNumber("Enter image height (y) ", 480);
```

```
w = w/2;
h = h/2;

//Loop through the images in the folder and extract interested values
for (z=0; z<list2.length; z++) {
open(dir2+list2[z]);        //opens every image
showProgress(z+1, list2.length);

        start = getTime();        // Get current time for progress bar

//calculate RGB
subloop=0;
while(subloop<10)
{
w2 = w-15 + 30*random();
h2 = h-15 + 30*random();

        v = getPixel(w2, h2);
        r = (v & 0xff0000)>>16;
        g = (v & 0x00ff00)>>8;
        b = (v & 0x0000ff);

                if(r<80){
        setResult("R", row, r);
        setResult("G", row, g);
        setResult("B", row, b);

//calculate CMYK

        c = 1.0 - r/255;
        m = 1.0 - g/255;
        y = 1.0 - b/255;
```

```
        k = minOf3( c, m, y);
        if ( k == 1.0 ) {
                c = m = y = 0;
                }
        else {
                s=1.0 - k;
                c = ( c - k ) / s;
                m = ( m - k ) / s;
                y = ( y - k ) / s;
        }

        setResult("C", row, c);
        setResult("M", row, m);
        setResult("Y", row, y);
        setResult("K", row, k);

//calculate HSV and HSL

        rScale = r/255;
        gScale = g/255;
        bScale = b/255;

        M = maxOf3(rScale, gScale, bScale);
        m = minOf3(rScale, gScale, bScale);

        r = (M - rScale) / (M - m);
        g = (M - gScale) / (M - m);
        b = (M - bScale) / (M - m);

        V = maxOf3(rScale, gScale, bScale);
        L = ( M + m) / 2;
```

```
if ( M == 0 ) {
        S = 0;
        S2 = 0;
        H = 180;
}
else {
        S = (M - m) / V;
        S2 = (M - m) / (1 - abs(2*L - 1));
}

if ( rScale == M ) {
        H = 60*(b-g);
}
if ( gScale == M ) {
        H = 60*(2+r-b);
}
if ( bScale == M ) {
        H = 60*(4+g-r);
}
if ( H>= 360 ) {
        H = H - 360;
}
if ( H< 0 ) {
        H = H + 360;
}

setResult("H", row, H);
setResult("S", row, S);
setResult("V", row, V);
setResult("S2", row, S2);
setResult("L", row, L);
```

```
            setResult("x", row, w2);
            setResult("y", row, h2);
            setResult("pic",row,pic);
            setResult("subloop", row, subloop);
            row++;  //increment the row for each image
            subloop++;
            }//end if
  }// end while
pic++;
            //updateResults();
saveAs("Results", dir3+"imageData.txt");
 }// end for
```

Appendix B

The blood was dropped onto different objects in the bedroom, bathroom and terrace such as cotton cloth, denim, leather bag, plastic cup, plastic dish, tile dish, canvas shoe, white paper, stainless fence, flagstone and wall. The samples were naturally exposed to different environmental conditions including heat and light.

Appendix B. Figure 1 Bloodstains of the mock casework experiment.

Forensic Science International 233 (2013) 288–297

Contents lists available at ScienceDirect

Forensic Science International

journal homepage: www.elsevier.com/locate/forsciint

Age estimation of bloodstains using smartphones and digital image analysis

Phuvadol Thanakiatkrai *, Alisa Yaodam, Thitika Kitpipit

Forensic Science Program, Department of Applied Science, Faculty of Science, Prince of Songkla University, Hat Yai, Songkhla 90112, Thailand

ARTICLE INFO

Article history:
Received 27 July 2013
Received in revised form 26 September 2013
Accepted 30 September 2013
Available online 9 October 2013

Keywords:
Forensic science
Hemoglobin
Color analysis
Digital image analysis
Random Forests

ABSTRACT

Recent studies on bloodstains have focused on determining the time since deposition of bloodstains, which can provide useful temporal information to forensic investigations. This study is the first to use smartphone cameras in combination with a truly low-cost illumination system as a tool to estimate the age of bloodstains. Bloodstains were deposited on various substrates and photographed with a smartphone camera. Three smartphones (Samsung Galaxy S Plus, Apple iPhone 4, and Apple iPad 2) were compared. The environmental effects – temperature, humidity, light exposure, and anticoagulant – on the bloodstain age estimation process were explored. The color values from the digital images were extracted and correlated with time since deposition. Magenta had the highest correlation ($R^2 = 0.966$) and was used in subsequent experiments. The Samsung Galaxy S Plus was the most suitable smartphone as its magenta decreased exponentially with increasing time and had highest repeatability (low variation within and between pictures). The quantifiable color change observed is consistent with well-established hemoglobin denaturation process. Using a statistical classification technique called Random Forests™, we could predict bloodstain age accurately up to 42 days with an error rate of 12%. Additionally, the age of forty blind stains were all correctly predicted, and 83% of mock casework samples were correctly classified. No within- and between-person variations were observed ($p > 0.05$), while smartphone camera, temperature, humidity, and substrate color influenced the age determination process in different ways. Our technique provides a cheap, rapid, easy-to-use, and truly portable alternative to more complicated analysis using specialized equipment, e.g. spectroscopy and HPLC. No training is necessary with our method, and we envision a smartphone application that could take user inputs of environmental factors and provide an accurate estimate of bloodstain age.

1. Introduction

Blood is commonly found in violent crimes such as homicides and assaults. Forensic scientists can acquire diverse information from bloodstains, e.g. sequence of events using blood pattern analysis and DNA profiles for individualization. Knowing the time since deposition of bloodstains can provide additional information to the investigators, as this can corroborate an eyewitness's account; narrow the time window for a missing person inquiry, kidnapping, and crimes without any eyewitness; and exclude bloodstains that are irrelevant to the crime.

Bloodstain age estimation dates back to over 50 years ago, and was based on spectrophotometric observation of bloodstain's color change from red to dark brown [1]. Since then researchers have tried numerous techniques to estimate time since deposition of bloodstains, including RNA analysis [2], high performance liquid chromatography [3], force spectroscopy [4], near-infrared spectroscopy [5], UV–vis spectroscopy [6,7], reflectance spectroscopy [8,9], and hyperspectral imaging [10,11]. Despite the revival of research interest in this area in recent years, estimating bloodstain age has not been implemented in routine crime scene investigations. The problem lies in the complex procedures requiring specialist knowledge, low accuracy and precision, and sophisticated, expensive machines. Spectroscopy-based techniques and hyperspectral imaging are the closest to being implemented due to their widespread availability and portability [7].

Once blood leaves the body, hemoglobin (the iron-containing oxygen transport protein in red blood cells) undergoes a non-reversible decay process: (1) rapid saturation of oxy- and deoxy-hemoglobin with oxygen in the atmosphere to form oxy-hemoglobin (2) oxy-hemoglobin auto-oxidizes into met-hemoglobin in the absence of cytochrome *b5* reductase (3) met-hemoglobin then denatures into hemichrome [12]. This is accompanied by the change of color from red to dark brown. The rate of change depends on environmental factors such as exposure to light, temperature,

* Corresponding author. Tel.: +66 74288565; fax: +66 74446681.
E-mail addresses: pthanakiatkrai@gmail.com, phuvadol.t@psu.ac.th (P. Thanakiatkrai).

0379-0738/$ – see front matter © 2013 Elsevier Ireland Ltd. All rights reserved.
http://dx.doi.org/10.1016/j.forsciint.2013.09.027

and humidity [12,13]. Since this change is temporally dependent, the amount of these derivatives has been used for estimating time since deposition of bloodstains [9–11].

As the phenomenon is observable with the naked eyes, we expected the color change to be quantitatively detectable in a digital image of the bloodstains. A digital image is formed when an image sensor converts reflected light that has passes through three color filters – red, green, and blue (RGB) – into digital signals. The intensity of the RGB values determines the final color of each pixel (the smallest element in a display device). We hypothesized that these values and their counterparts, e.g. cyan, magenta, yellow, and key (CMYK), can be plotted against time since deposition to generate a calibration curve; subsequently, the time since deposition of unknown samples can be determined by comparing their color values to the calibration curve. A similar process has been used to correlate the color change of chicory to storage time [14], as well as to determine the concentration of amphetamine, methylamphetamine [15], and trinitrotoluene (TNT) [16,17].

In this study, we used digital image analysis of bloodstains to estimate the time since deposition and evaluated the effects of smartphone camera, person-to-person variation, temperature, humidity, light exposure, anticoagulant, and substrate on the estimation process. Our proposed technique requires only a digital camera and a computer, both of which are readily available in any forensic laboratory. A smartphone application can be developed to carry out the technique proposed at crime scenes, making this method low-cost, simple, rapid, and truly portable.

2. Materials and methods

2.1. Sample collection

Blood samples were collected from four volunteers to assess person-to-person variation and blind test and only from one volunteer for all other experiments (as recommended by Bremmer et al. [13]) using procedures approved by the Prince of Songkla University Ethical Committee (ethical approval no. 56-293-19-2). Informed written consents were obtained from all volunteers. Three female and one male volunteers donated blood. All volunteers were Asian, healthy, non-smoker, and ate a normal diet. None of the females were menstruating at the time of blood collection. The mean age was 23.5 ± 2.4 years. Venous blood was collected from venipuncture into an additive-free microcentrifuge tube.

All bloodstains were made with 50 μl of blood and kept in the dark at 25 °C except for the light exposure study, temperature study, and mock casework test. The time between blood collection and deposition onto substrates was less than 30 s. Five bloodstains were deposited for each study unless otherwise stated:

- Color value selection and within-/between-person variation: bloodstains from four individuals on filter paper.
- Smartphone: bloodstains on filter paper taken with three smartphone cameras (iPhone 4, iPad 2, and Samsung Galaxy S Plus).
- Temperature: bloodstains on filter paper kept at −20 °C, 4 °C and 25 °C.
- Humidity: bloodstains on filter paper at room temperature with 30% and 50% relative humidity.
- Light exposure: bloodstains on filter paper kept under direct sunlight, fluorescent lamp, and in the dark.
- Anticoagulant: blood samples collected in 1.5 mg ethylene diamine tetra acetic acid (EDTA), 0.2 mg of heparin, and no anticoagulant on filter paper.
- Substrate: bloodstains on denim, filter paper, glass, gypsum board, leather, and white cotton.
- Blind test: 40 bloodstains deposited on filter paper. Four stains were randomly chosen, assigned a random five-digit identifier code, and frozen at −80 °C at 15 min, 30 min, 1 h, 6 h, 1 day, 3 days, 7 days, 14 days, 28 days, and 42 days.
- Mock casework: 24 bloodstains deposited randomly on household objects – white A4 paper, gray stone slab floor, white plastic dish, white sneakers, white t-shirt, and cream leather handbag. Temperature and humidity were not controlled in this study. Eight samples were randomly chosen and frozen at −80 °C at the age of less than one day, another eight between one day and one week, and the last eight between one week and one month.

2.2. Photographic system

We set up a simple, low-cost photographic system consisted of a white foam light box (2666 cm^2 inner surface area) illuminated evenly with a Sylvania Osram DULUX S 9-Watt Cool White bulb (G32-2 pin base, 600 lumens, 4100K color temperature, Sylvania Osram, Thailand). Fig. 1 shows a schematic drawing of the light box. The fluorescent lamp output all wavelengths of the visible spectrum, from 350 nm to 750 nm [18]. On top of the box was a hole just big enough for a smartphone camera lens to fit.

A Samsung Galaxy S Plus was used to capture digital images (five images per stain) of the bloodstains in all studies except in the smartphone study. Five photographs were taken from each stain to account for variations in precision due to experimental errors, such as inhomogeneous lighting and flickering of the fluorescent lamp. Images were taken at 15 min, 30 min, 1 h, 3 h, 6 h, 12 h, 1 day, 2 days, 3 days, 4 days, 5 days, 6 days, 1 week, 2 weeks, 4 weeks, 6 weeks, 2 months, 3 months, 4 months, 5 months, and 6 months. For blind testing, we photographed all the previously frozen stains on the 42nd day. All settings were set to automatic (white balance, ISO, focusing mode, and metering mode). The file type selected was 24-bit JPEG and the resolution was 2592 × 1944, 2592 × 1936, and 960 × 720 pixels for the Samsung Galaxy S Plus, iPhone 4, and iPad 2, respectively. The color intensity in four color models (RGB, CMYK, HSV, HSL) of each image were extracted using an ImageJ macro (http://imagej.nih.gov) that we developed. The macro randomly selected ten pixels of the bloodstain and averaged their color values. The color values were then exported to R statistical program (http://cran.r-project.org) for further analysis.

2.3. Statistical analysis

We transformed the time since deposition using base-10 logarithm to linearize the relationship between color values and time (in hours). Outliers were discarded prior to further statistical analysis. We then applied a linear regression to each color value and time and determine the correlation coefficient of each relationship. This was done to determine the best predictor for time since deposition. To estimate the effects of different donors, we used linear mixed modeling appropriate to the data collected.

For the smartphone, temperature, humidity, light exposure, and anticoagulant studies, we plotted the average (calculated from all photographs of all bloodstains unless stated otherwise) and 95% bootstrapped confidence interval of the magenta value at each time-point and fitted a local polynomial regression (LOESS) to reflect the biphasic change of hemoglobin derivatives. We concluded a significant difference when there was no overlap between the bootstrapped confidence intervals of the fit.

To determine the prediction accuracy of the method, we split the bloodstains of the person-to-person experiment into a training set (70% of data) and validation set (30% of data). Calibration curves were constructed using the data from the training set. The magenta values of bloodstains validation set were fitted to the training set calibration curve and their time since depositions were estimated. Moreover, we applied a machine learning process called Random Forests™ to predict time since deposition. The method constructed many decision trees (i.e. forest) from the bootstrapped samples of the training set (2/3 of the data) and used these forests to classify unknown samples in the validation set (1/3 of the data) [19]. In contrast to the calibration curve method, the Random Forests™ classification algorithm used more than one color values measured from the bloodstain images to classify their time since deposition. The out-of-bag (OOB) estimate of error rate represented the prediction error [19].

To further test the prediction accuracy of the Random Forests™ model built from the person-to-person variation study, we performed additional blind tests with 40 bloodstain samples and 24 mock casework samples. The actual ages of the samples and the estimated ages using the Random Forests™ model were compared to determine the prediction accuracy and estimation error. For the blind samples, the time-points used were the same with the person-to-person variation study. For the

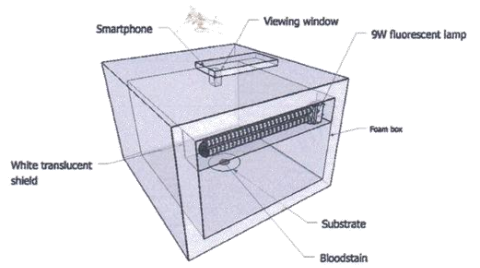

Fig. 1. 3D sketch of the photographic system used in this study. A Sylvania Osram DULUX S 9-Watt Cool White bulb was used to create an even illumination in the light box. Photographs were taken by placing a smartphone camera on the viewing window.

Table 1
Calibration curve equations from different color values of bloodstains from four donors. The two relationships with R^2 highest are bolded.

Parameter	Calibration equation	R^2
R and log time	$y = -6.0x + 81.6$	0.349
G and log time	$y = 6.48x + 25.6$	0.726
B and log time	$y = 3.78x + 25.2$	0.434
C and log time	$y = 0x + 0$	0.000
M and log time	**$y = -0.119x + 0.688$**	**0.966**
Y and log time	$y = -0.0843x + 0.696$	0.896
K and log time	$y = 0.0235x + 0.680$	0.349
H and log time	$y = -41.1x + 98.9$	0.224
S and log time	**$y = -0.0843x + 0.531$**	**0.911**
L and log time	$y = -0.00392x + 0.209$	0.026

mock casework samples, only a rough estimation window was used: less than one day old, between one day and one week old, and more than one week old.

3. Results

A new method to determine the time since deposition of bloodstains through digital image analysis using a smartphone camera was devised. The results indicate that bloodstain color changes with time and this change is quantifiable using digital image analysis. Many factors affected the color values, including smartphone camera, temperature, humidity, light exposure, the addition of anticoagulant, and substrate color.

3.1. Color value selection and within- and between-person variation

We compared the correlation coefficient of each color value in all color models with time since deposition. M (magenta in CMYK) and S (saturation in HSL) correlated highly with time since deposition with R^2 values of 0.966 and 0.911 (Table 1) using linear modeling. The decrease in these color values followed a logarithm decay pattern – rapid decrease in the beginning followed by a slow decrease at later time-points (Fig. 2). The first two time-points (15 and 30 min) and the time-points over 6 weeks were excluded from the linear models, as the decrease in color values in the first hour was even more rapid than a logarithmic function. Additionally, magenta values of bloodstains after 6 weeks did not decrease any further (data not shown). Magenta was selected for further studies due to its high correlation with time since deposition.

Fig. 2(top) displays the within-person variation and Fig. 2(bottom) shows the between-person variation with passing time. Again, the main trend is the biphasic decrease in magenta values. Only minimal variations were observed within-person, as indicated by the clustering of the magenta values from the five bloodstains of each donor. Linear mixed model with time since deposition as a fixed effect and with donor and bloodstain nested within donor as random effects showed that bloodstain was not significant ($p > 0.05$), i.e. there was no within-person variation. As for between-person variation, the overlap in the confidence

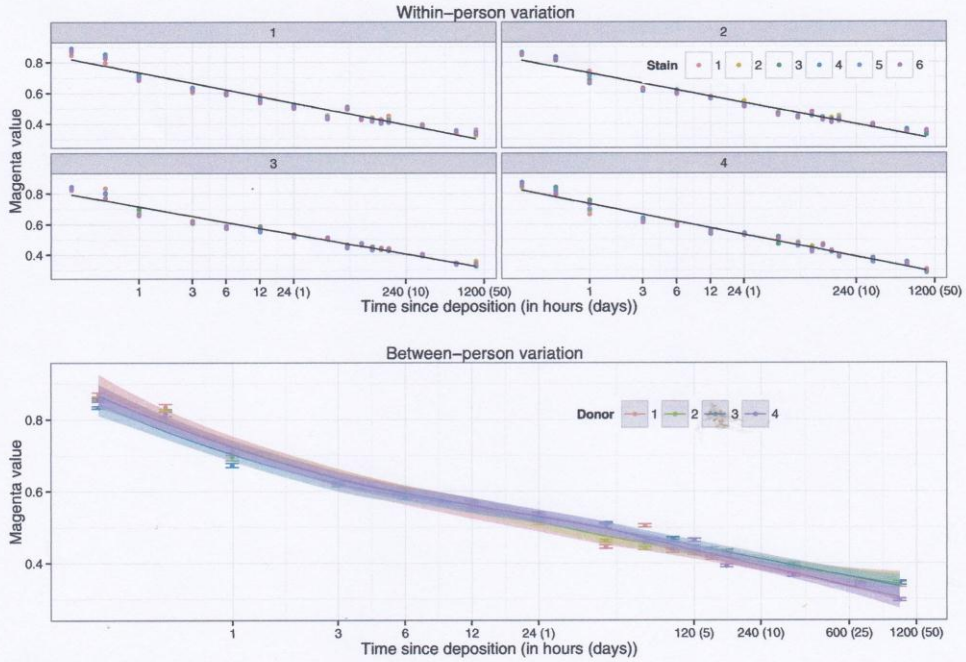

Fig. 2. Top: The change in magenta value of each bloodstain ($N = 5$) for each donor ($N = 4$) and the line of best fit. Each bloodstain was photographed five times and only the average of the five photographs is plotted. Bottom: Average and 95% confidence intervals of magenta values obtained from five bloodstains of each donor. The overlapped LOESS confidence intervals suggest no person–person variation. (For interpretation of the references to color in this figure legend, the reader is referred to the web version of this article.)

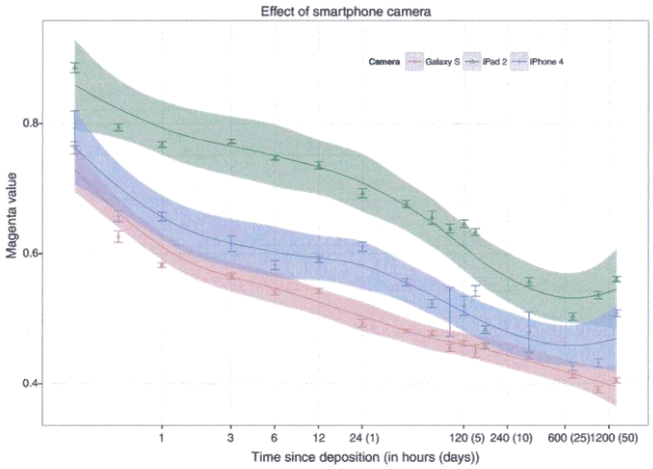

Fig. 3. Average and 95% confidence intervals of magenta values obtained from bloodstains ($N = 5$ for each smartphone) using three smartphone cameras. Only Samsung Galaxy S Plus provided high repeatability (narrow confidence intervals at all time-points) and a consistently decreasing trend. (For interpretation of the references to color in this figure legend, the reader is referred to the web version of this article.)

interval of each donor's LOESS fit suggests that there was no person-to-person variation. We also constructed a linear mixed model with time since deposition as a fixed effect and donor as a random effect. Only time since deposition was statistically significant ($p < 0.001$). The variation in magenta due to different donors was less than 2% of the total variation and thus not statistically significant.

3.2. Smartphone camera comparison

Three different smartphone cameras were compared to determine the most suitable camera for bloodstain age estimation. The Samsung Galaxy S was the most suitable smartphone, as evidenced by its narrow 95% bootstrapped confidence interval and non-fluctuating color values (Fig. 3). The Apple iPad 2 and iPhone 4

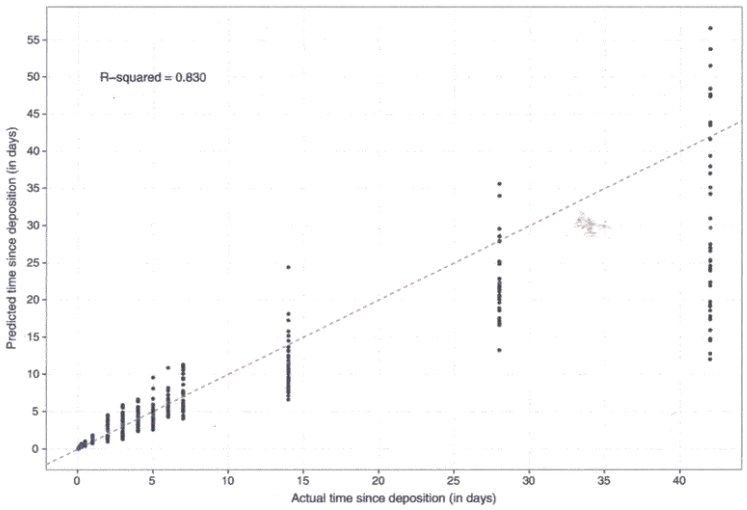

Fig. 4. Predicted age of bloodstains versus the actual age. Means are shown as blue dots. The line of unity is plotted as a dashed red line. The adjusted R-squared of the relationship was 0.830. (For interpretation of the references to color in this figure legend, the reader is referred to the web version of this article.)

Table 2
The confusion matrix using Random Forests™ person-to-person variation experiment. Figure in bold refers to the number in each group correctly classified.

	Predicted														
Actual	1 h	3 h	6 h	12 h	1 d	2 d	3 d	4 d	5 d	6 d	7 d	14 d	28 d	42 d	Error
1 h	**109**	11													9%
3 h	10	**110**													8%
6 h		1	**119**												1%
12 h			1	**107**	12										11%
1 d				13	**96**	11									20%
2 d					17	**89**	13	1							26%
3 d						12	**93**	14	1						23%
4 d						2	13	**91**		2		12			24%
5 d							1	1	**106**	3	9				12%
6 d								2	7	**96**	8	7			20%
7 d									7	8	**100**	3		2	17%
14 d								6		1		**108**	4	1	10%
28 d								1		1		1	**116**		3%
42 d											3			**114**	5%

cameras displayed fluctuating magenta values with increasing time; thus, both were not suitable for predicting time since deposition. Using linear models, magenta values had the highest correlations with all three smartphones. Galaxy S Plus had a correlation coefficient of 0.935, followed by 0.796 of iPhone 4, and 0.637 of iPad 2. Based on these two reasons – no fluctuation and high correlation with time since deposition, the Samsung Galaxy S Plus was selected for further studies.

3.3. Bloodstain age estimation using linear regression and Random Forests™

We used the data from the person-to-person variation study to assess prediction accuracy for unknown stains. 2160 bloodstain images were divided into two sets – training set (70%) and validation set (30%). A simple age estimation method using linear regression with magenta value as the predictor for time since deposition gave highly accurate and precise predictions up to one day, but both accuracy and precision worsened with increasing time (Fig. 4).

A more complicated machine learning classification algorithm called Random Forests™ [19] was then applied to use information from all color values to obtain a more accurate prediction. We constructed 1000 classification trees using all the color values as predictors with the number of variables tried at each decision split set to six. The results are shown in Table 2. As expected, more accurate predictions were obtained using more color values. The overall out-of-bag (OOB) error rate (i.e. the prediction error for Random Forests™) was 12%, with lower error rates for the very early and late time-points. It was possible to predict the time since deposition of bloodstains very accurately using this method. For example, 119 of 120 stains were correctly classified for the stains at 6 h after deposition.

Random single blind trial was performed with forty new bloodstains on filter paper using the same data collection equipment and protocols. The previously built Random Forests™ model was used to predict the age of these forty samples. All samples were correctly classified at all time-points (15 min, 30 min, 1 h, 6 h, 1 day, 3 days, 7 days, 14 days, 28 days, and 42 days). In other words, 100% estimation accuracy was obtained with blind samples.

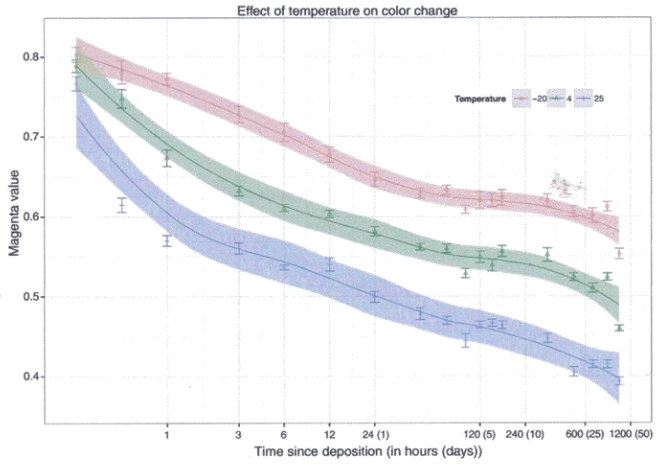

Fig. 5. Average and 95% confidence intervals of magenta values obtained from bloodstains ($N = 5$ for each temperature) kept at −20 °C, 4 °C, and 25 °C. Higher temperature increased the rate of hemoglobin denaturation. (For interpretation of the references to color in this figure legend, the reader is referred to the web version of this article.)

We further investigated whether the model built using data from bloodstains on filter paper could be used to roughly estimate the age of bloodstains on other substrates in an uncontrolled environment. The estimation categories were (1) less than one day old, (2) between one day and one week old and (3) more than one week old. Twenty-four mock casework stains deposited on white A4 paper, gray stone slab, white plastic dish, white sneakers, white t-shirt, and cream leather handbag showed that 7 of 8 stains were correctly classified to less than one day, 5 of 8 stains were correctly classified to between one day and one week, and all 8 stains were correctly classified to more than one week old. Overall, using these three age groups achieved 83% prediction accuracy for uncontrolled mock casework stains.

3.4. Environmental effects on the aging process

3.4.1. Temperature

Temperature affected the color change process of bloodstains. The three storage temperatures tested (−20 °C, 4 °C, and 25 °C) produced a different pattern in magenta values (Fig. 5). For the samples kept at 4 °C and 25 °C, magenta value rapidly decreased during the first hour followed by a gradual decrease. This pattern was not seen in the samples kept at −20 °C. The 95% bootstrapped confidence intervals did not overlap at any time-point except at the 15-min mark.

3.4.2. Humidity

Two humidity levels were compared: 30 and 50 (%RH) and was found to have a significant effect on the color change process. The level of magenta decreased more rapidly in the earlier time-points at 30%RH when compared with 50%RH (Fig. 6). There were small overlaps in the 95% confidence interval of the two sets of bloodstains exposed to different humidity levels between 3 and 24 h. The two confidence intervals split after that and re-overlapped after one month.

3.4.3. Light exposure

Exposure to sunlight produced a different color change pattern when compared with bloodstains kept in the dark and under fluorescent light in Fig. 7. At 15 min, we observed a difference between bloodstain samples stored in the dark and exposed to light (both fluorescent light and sunlight). At 30 min, bloodstains exposed to sunlight had significantly lower magenta values than bloodstains kept in the dark and exposed to fluorescent light. After one hour, bloodstains kept in the dark and under fluorescent light were indistinguishable. The samples exposed to sunlight had their colors changed faster in the early hours (larger drop in magenta value). The LOESS fits of the three exposure conditions overlapped consistently after one day.

3.4.4. Anticoagulant

The two anticoagulants tested did not affect the magenta value of the bloodstains in Fig. 8. We observed considerable overlaps in the 95% bootstrapped confidence intervals between the control bloodstains and the anticoagulant-mixed bloodstains. The only difference seemed to be from three to twelve hours after deposition, where the control bloodstains exhibited higher magenta values.

3.5. Effect of substrate and substrate color

Only lightly colored substrates exhibited high correlation with the magenta value (filter paper, cream leather, and white cotton). Fig. 9 shows highly similar color change patterns with these three substrates. On the other hand, the magenta values of bloodstains on blue denim, clear glass, and gray gypsum board had poor correlation with time since deposition. Denim's blue color interfered with the magenta's color of the bloodstains. Glass did not absorb bloodstains and caused the stains to crust into varying thickness, which interfered with the color change and the color measurement process. Gypsum's gray color also interfered with

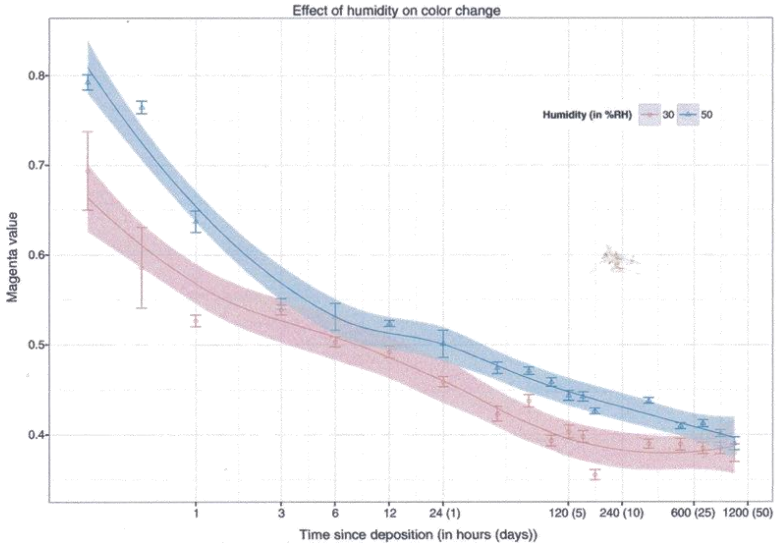

Fig. 6. Average and 95% confidence intervals of magenta values obtained from bloodstains ($N = 5$ for each humidity level) kept at 30% and 50% relative humidity at 25 °C. Higher humidity slowed the color change process. (For interpretation of the references to color in this figure legend, the reader is referred to the web version of this article.)

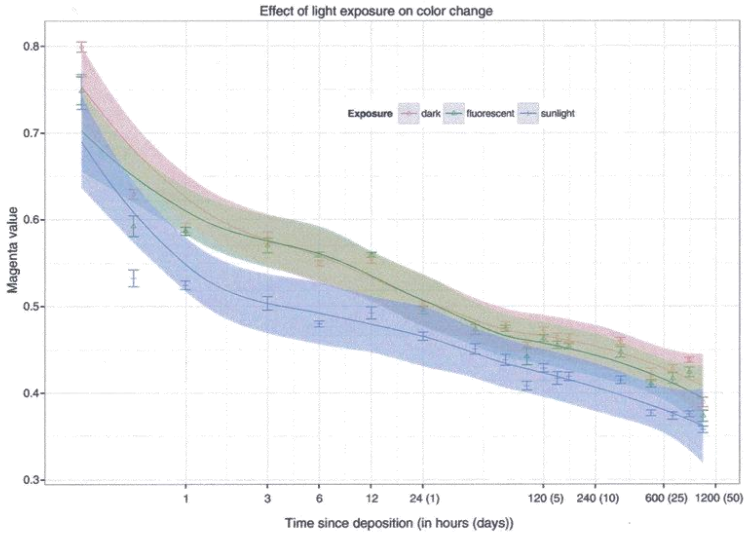

Fig. 7. Average and 95% confidence intervals of magenta values obtained from bloodstains ($N = 5$ for each condition) kept in the dark, under fluorescent lighting, and under natural sunlight. No difference was observed for the bloodstains in the dark and under fluorescent light. (For interpretation of the references to color in this figure legend, the reader is referred to the web version of this article.)

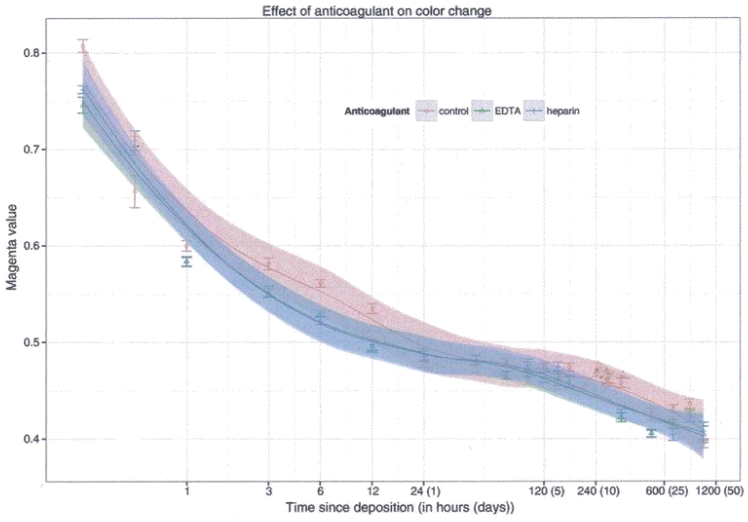

Fig. 8. Average and 95% confidence intervals of magenta values obtained from control bloodstains, bloodstains mixed with EDTA, and bloodstains mixed with heparin ($N = 5$ for each). Anticoagulants did not affect the color change process. (For interpretation of the references to color in this figure legend, the reader is referred to the web version of this article.)

the color measurement. Furthermore, in the first hour after deposition, bloodstains were not absorbed into the gypsum and this non-uniformity in thickness affected the color change process.

4. Discussion

We found that color values from digital image can predict time since deposition of bloodstains. To the best of our knowledge, this

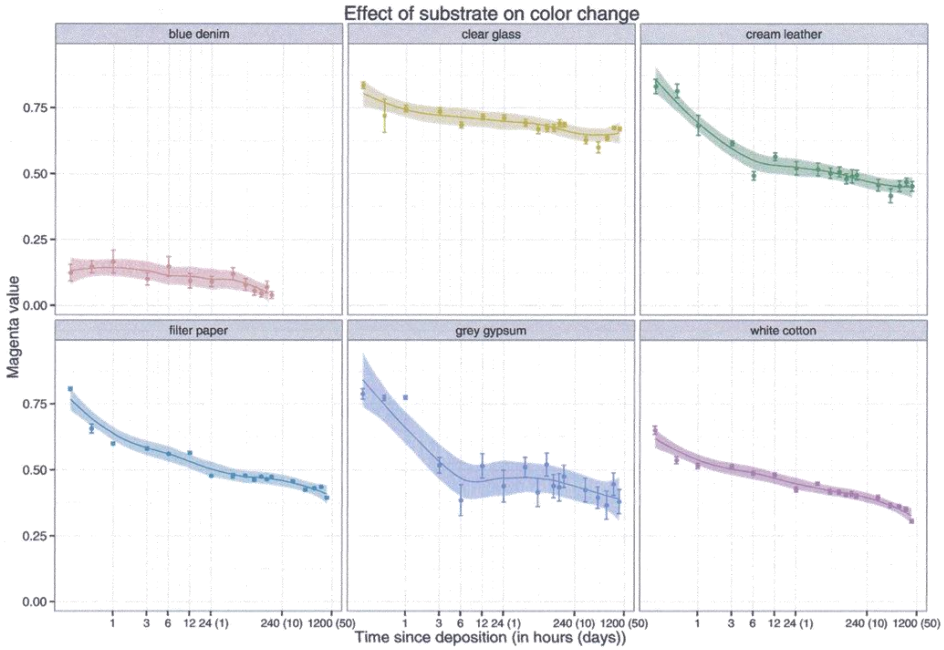

Fig. 9. Average and 95% confidence intervals of magenta values from bloodstains ($N = 5$ for each substrate) deposited onto six substrates. Only bloodstains on white or lightly colored substrates displayed high correlation of magenta values with increasing time since deposition. (For interpretation of the references to color in this figure legend, the reader is referred to the web version of this article.)

is the first time a smartphone camera is used for such purposes. The change in color of bloodstains depended on many factors, e.g. humidity, temperature, and light exposure. Smartphone cameras and their color correction algorithms also influenced the process, as different color values were obtained from the same bloodstains. Our proposed technique is cheap, truly portable, accurate, and quick, requiring only a smartphone camera, a dedicated light box, and a computer. As such, it can be easily adopted for crime scene use.

In Random Forests™, there is no need to perform additional cross-validation to obtain an unbiased estimate of error, as the estimate of error is performed internally. Each classification tree is constructed using two-third bootstrapped data. These trees are then used to classify the other one-third of the data and the process repeated many times to obtain an out-of-bag estimate of error [19,20]. Our OOB error compares favorably against other published methods. Two most recent studies using hyperspectral imaging obtained an error rate of about 40% for the whole 30 days [11] and 13.4% for up to 200 days [10]. Ours was 12% for up to 42 days using the Random Forests™ method. It must be noted that Edelman et al. and Li et al. collected data at a scale that is finer than us and that could be why our error rate is slightly lower. However, our method was much simpler because we did not need a hyperspectral imaging system and high computing power. The 100% prediction accuracy with blind samples further affirms that the proposed method has potential to be improved upon and validated. Even with mock casework samples of unknown age in an uncontrolled environment, the Random Forests™ model built on controlled stains were able to roughly categorized bloodstains into three age groups with reasonably high accuracy.

The limitation of classification-based methods such as the Random Forests™ method used here or the linear discriminant analysis (LDA) method used by other researchers [11,26] is its categorical nature, i.e. a bloodstain could only be classified to a time-point that has been used to build the model. A regression-based method might be more appropriate as bloodstain age could be predicted in minutes instead, which reflects its continuous nature. Alternatively, measurements could be at frequent time intervals (e.g. Li et al. [11] collected data every hour for the first day and every day for 30 days) to increase the categories available for prediction. In a classification model, probabilities could be assigned to different time-points for each group of bloodstains as a way to present the uncertainties of the estimate. A Bayesian credible interval or a frequentist confidence interval could be used for a regression-based method.

Overall, the main advantages of our technique are convenience and cost. Our proposed method is the easiest to implement because no specialized equipment is needed, i.e. only a smartphone whose price is about 200 USD, weighs less than 120 g, and only 12 cm long. The light box is made from a re-used foam box equipped with a 20 USD lamp, as compared to the 2000 USD solid state plasma light source used by Li et al. [11]. Other recent studies with spectroscopy did not provide numerical data in their validation of prediction accuracy; thus, we could not compare our results to theirs [7,9].

4.1. Color change and photographic systems

Hemoglobin makes up 97% of blood's dry content; thus, it is the major chromophore in blood. The color of the bloodstain is determined by the ratio of three hemoglobin derivatives (oxy-hemoglobin, met-hemoglobin, and hemichrome) in the bloodstain, since each derivative has a unique absorption spectrum [12]. The fraction of each hemoglobin derivative changes with time. The process is described as biphasic: a rapid auto-oxidation of oxy-hemoglobin in the first few hours and the slow denature of met-hemoglobin to hemichrome [12]. We did not test our method with capillary or arterial blood, because blood from any source will be fully saturated with oxygen upon exiting the body as all bloodstains are exposed to the oxygen in the environment [9]. In other words, although venous blood is darker inside the body due to the higher percentage of deoxyhemoglobin in the red blood cells of venous blood, all deoxyhemoglobin will change to oxyhemoglobin once blood leaves the body; thus all fresh blood will turn bright red regardless of its source.

The color change due to this denaturation process was quantifiable using a smartphone camera followed by color analysis in our study. The change in some color values, e.g. magenta and saturation values, correlated well with time since deposition.

All digital images are formed from three 8-bit channels: red, green, and blue. The values of RGB range from 0 to 255. RGB can be converted to other color spaces such as CMYK (cyan, magenta, yellow, key) and HSL (hue, saturation, lightness). The change in color of blood from bright red to dark brown can be summarized in RGB terms as follows: the difference between red (255, 0, 0) and brown (150, 75, 0) is the decrease in R channel and increase in G channel. This simultaneous decrease in red and increase in green could also be described by magenta color, which is the combination of red and blue (i.e. the complementary of green).

Although the iPhone's back-illuminated sensor technology allows more light to hit the sensor by repositioning the wiring [16], the improved sensitivity to light did not improve the results obtained when compared to the smaller, older image sensor in the Galaxy S Plus camera. This could be due to the evenly lit and bright light box as well as the software-based color correction algorithms. The bright conditions must have negated the need for a bigger sensor. While human sees the same color from an object under different lights, digital cameras cannot do so and relies on these algorithms to correct for the differences [21]. Unlike the RAW format from a digital single-lens reflex (DSLR) camera, a compressed JPEG file from smartphone cameras has undergone image processing, including color correction. Our results suggest that the three smartphones used different algorithms for color balancing, as pictures of the same bloodstains gave different color values. The goal of a smartphone camera is to produce a good-looking image with the least user effort required. Apple Inc., the maker of iPad 2 and iPhone 4, has patents pertaining to image processing related to color correction (e.g. [22,23]) and these could have affected the color values of the bloodstains.

A simple, truly low-cost light box was built to achieve an even and consistent illumination throughout the experiment. Illumination intensity affects the color of the photographs directly and thus it must be controlled. We used a household lamp with a Sylvania Osram 9-Watt light bulb that outputs all wavelengths in the visible spectrum [18]. Our results demonstrate that even a normal fluorescent light bulb, which costs less than 10 USD and is over 500 times cheaper than a standard light emission system (e.g. Thorlabs HPLS-30-02 solid state plasma light source used by Li et al. [11]), produce a consistent, accurate result. A box like ours could be carried to a crime scene and used there to standardize the illumination *in situ*. Improvements to the box can certainly be made, e.g. modifying the box so that it covers a stain directly without letting any outside light in; thus the only illumination source is the light bulb installed in the box. Other light sources could also be tried, such as LEDs, to explore specific wavelengths that might be more appropriate for our method.

4.2. Environmental effects

The rapid color change with higher temperatures in our results confirmed that high temperature increases the rates of change from oxy-hemoglobin to met-hemoglobin and from met-hemoglobin to hemichrome [12]. We also found that higher humidity slows the color change process, in agreement with Bremmer et al. who reported that increased humidity slows down the change from met-hemoglobin to hemichrome [12].

Conflicting reports of the influence of light exposure were found in the literature and seemed to be method-specific [7,24,25]. In our case, we observed highly similar degradation pattern between bloodstains stored in the dark and under fluorescent light, while the bloodstains kept under natural sunlight changed color faster. However, this higher rate of change could be due to the difference in temperature and humidity that the bloodstains were exposed to. The bloodstains kept under natural sunlight were not kept in the same room with the other two sets. Direct exposure to sunlight also raised the temperature of the air and the substrate, which further confounded our results.

EDTA and heparin did not affect the color change of bloodstains in our study. No evidence in the literature was found about the influence of anticoagulants on the aging process of bloodstains [13]. The effects of temperature, humidity, and light exposure must be considered when applying the technique used in this study. Further studies must be conducted to validate different smartphones and light sources for each temperature and humidity combination.

Bloodstain thickness was not directly investigated but it could have influenced the age estimation process. The bloodstains on glass, a non-absorbent surface, were initially spread out but gradually formed a thick clump as they dried. Clumping of bloodstains probably had a two-fold influence: slowing the exposure of hemoglobin to light, humidity, and temperature and changing the color of bloodstain due to the longer light path. Other substrates absorbed blood and formed a thin stain of about 0.1 mm. The slight variations in thickness presented was overcome by the sampling process used in this study, which was to extract color values from ten pixels from each of the five photographs of a single stain.

We used 50 μl of blood in our study. This produced a bloodstain of approximately 20 mm in diameter on filter paper, which translated to over 50,000 pixels in a 5-megapixel digital image. We randomly chose only ten pixels around the center area of the stain and this was sufficient for an accurate estimate of bloodstain age. Accounting for capillary flow, which makes a stain thicker around the edge [9], we estimated that a 5-μl bloodstain should still have around 500 pixels available for analysis. Even a 1-μl bloodstain should still have around 100 pixels available.

4.3. Substrate material and color

In an actual crime scene, it is impossible to dictate the color of the substrate that bloodstains will be deposited and other environmental conditions. Our results suggest that colored substrates interfere with the color of the bloodstains. Magenta values of lightly colored substrates correlated well with time since deposition but for dark or non-absorbent substrates (e.g. jeans, dark cotton, and glass) it was nearly impossible to see the bloodstains. Color correction or normalization of color values using background color did not improve the prediction process (data not

shown). For bloodstains deposited indoors, the temperature and humidity levels tend to be stable and an average could be used for the prediction process. For bloodstains exposed to the environments such as fluctuating temperature and sunlight, Hanson and Ballantyne suggested that only a crude approximation to time since deposition could be made [7]. In countries like Thailand where the average outdoor temperature, average outdoor humidity level, and the hours of sunlight are relatively stable day-to-day, better prediction accuracy is expected. Validation of the method for each area is necessary before implementation.

As the substrate color interferes with the color detection process, extraction of bloodstains from substrate could be useful as an adjunct to this method. Hanson and Ballantyne pre-extracted the bloodstains in TBE buffer and successfully used UV–vis spectrophotometry to correlate bloodstains' spectrograph with time since deposition [7]. We are currently investigating a similar extraction method. Alternatively, infrared wavelengths could also be useful for colored substrates. Near-infrared and mid-infrared spectrographs of bloodstains have been shown to circumvent the limitation of a white background [5]. A digital camera can be modified to capture the infrared wavelengths and its usability in bloodstain age estimation is currently being explored.

We demonstrated that our technique was highly accurate under controlled conditions and that there were minimal within- and between-person variations. This makes our proposed technique worthy of further investigation. The conditions of an actual crime scene cannot be predicted beforehand and will undoubtedly decrease the prediction accuracy. We showed that the method has potential through rough estimation of mock casework stains under uncontrolled conditions. A better prediction model can be achieved through a large-scale controlled study using a full factorial design to simultaneously evaluate the influence and the interactions of temperature, humidity, light, stain size, substrate color, smartphone, and illumination system. These effects could then be parameterized and higher prediction accuracy could be obtained. We have demonstrated that bloodstain age estimation on white substrates is possible but further optimization and validation with other substrates in a large-scale study needs to be done before the method is accepted in the court of law.

5. Conclusions

This study is the first time a smartphone camera has been used to predict the time since deposition of bloodstains. The quantifiable change in color due to the different ratios of hemoglobin derivatives can be simply detected using a smartphone. The smartphone brand, temperature, humidity, and light exposure affected the color change process. The two smartphone operating systems – Google's Android OS and Apple's iOS – have active developer communities and we envision a smartphone application that could give an estimate of the bloodstain age accurately in the near future. The application could request user input of smartphone brand, average temperature and humidity, whether the stain is indoor or outdoor, and factors them into the calculation. The application of smartphone cameras to bloodstain age estimation in actual crime scene warrants further investigation.

Author contribution

PT conceived of and carried out the study, analyzed the data, wrote the manuscript, and supervised the study. AY carried out the study and assisted with data analysis. TK designed the study, wrote the manuscript, and supervised the study.

Acknowledgements

This work was funded by the Faculty of Science Research Grant no. 156003, Prince of Songkla University. We acknowledge the help of the volunteers and Asst. Prof. Dr. Aree Choodum for her valuable comments regarding experimental set-up and discussion.

References

[1] D. Patterson, Use of reflectance measurements in assessing the colour changes of ageing bloodstains, Nature 187 (1960) 688–689.
[2] S.E. Anderson, G.R. Hobbs, C.P. Bishop, Multivariate analysis for estimating the age of a bloodstain, J. Forensic Sci. 56 (2011) 186–193.
[3] J. Andrasko, The estimation of age of bloodstains by HPLC analysis, J. Forensic Sci. 42 (1997) 601–607.
[4] S. Strasser, A. Zink, G. Kada, P. Hinterdorfer, O. Peschel, W.M. Heckl, A.G. Nerlich, S. Thalhammer, Age determination of blood spots in forensic medicine by force spectroscopy, Forensic Sci. Int. 170 (2007) 8–14.
[5] G. Edelman, V. Manti, S.M. van Ruth, T. van Leeuwen, M. Aalders, Identification and age estimation of blood stains on colored backgrounds by near infrared spectroscopy, Forensic Sci. Int. 220 (2012) 239–244.
[6] E. Hanson, A. Albornoz, J. Ballantyne, Validation of the hemoglobin (Hb) hypsochromic shift assay for determination of the time since deposition (TSD) of dried bloodstains, Forensic Sci. Int. Genet. Suppl. Series 3 (2011) e307–e308.
[7] E.K. Hanson, J. Ballantyne, A blue spectral shift of the hemoglobin soret band correlates with the age (time since deposition) of dried bloodstains, PLoS ONE 5 (2010) e12830.
[8] R.H. Bremmer, G. Edelman, T.D. Vegter, T. Bijvoets, M.C. Aalders, Remote spectroscopic identification of bloodstains, J. Forensic Sci. 56 (2011) 1471–1475.
[9] R.H. Bremmer, A. Nadort, T.G. van Leeuwen, M.J. van Gemert, M.C. Aalders, Age estimation of blood stains by hemoglobin derivative determination using reflectance spectroscopy, Forensic Sci. Int. 206 (2011) 166–171.
[10] G. Edelman, T.G. van Leeuwen, M.C. Aalders, Hyperspectral imaging for the age estimation of blood stains at the crime scene, Forensic Sci. Int. 223 (2012) 72–77.
[11] B. Li, P. Beveridge, W.T. O'Hare, M. Islam, The age estimation of blood stains up to 30 days old using visible wavelength hyperspectral image analysis and linear discriminant analysis, Sci. Justice 53 (2013) 270–277.
[12] R.H. Bremmer, D.M. de Bruin, M. de Joode, W.J. Buma, T.G. van Leeuwen, M.C. Aalders, Biphasic oxidation of oxy-hemoglobin in bloodstains, PLoS ONE 6 (2011) e21845.
[13] R.H. Bremmer, K.G. de Bruin, M.J. van Gemert, T.G. van Leeuwen, M.C. Aalders, Forensic quest for age determination of bloodstains, Forensic Sci. Int. 216 (2012) 1–11.
[14] M. Zhang, J. De Baerdemaeker, E. Schrevens, Effects of different varieties and shelf storage conditions of chicory on deteriorative color changes using digital image processing and analysis, Food Res. Int. 36 (2003) 669–676.
[15] A. Choodum, N.N. Daeid, Digital image-based colourimetric tests for amphetamine and methylamphetamine, Drug Test. Anal. 3 (2011) 277–282.
[16] A. Choodum, P. Kanatharana, W. Wongniramaikul, N. Nic Daeid, Using the iPhone as a device for a rapid quantitative analysis of trinitrotoluene in soil, Talanta 115 (2013) 143–149.
[17] A. Choodum, P. Kanatharana, W. Wongniramaikul, N. NicDaeid, Rapid quantitative colourimetric tests for trinitrotoluene (TNT) in soil, Forensic Sci. Int. 222 (2012) 340–345.
[18] Osram Sylvania, Spectral Power Distributions of Sylvania Fluorescent Lamps, Osram Sylvania, Massachusetts, USA, 2000.
[19] L. Breiman, Random forests, Mach. Learn. 45 (2001) 5–32.
[20] J.M. Hettick, M.L. Kashon, J.E. Slaven, Y. Ma, J.P. Simpson, P.D. Siegel, G.N. Mazurek, D.N. Weissman, Discrimination of intact mycobacteria at the strain level: a combined MALDI-TOF MS and biostatistical analysis, Proteomics 6 (2006) 6416–6425.
[21] J. Jiang, Y. Zhao, S-g. Wang, Color Correction of Smartphone Photos with Prior Knowledge. Imaging and Printing in a Web 20 World III, SPIE Proceedings, Burlingame, CA, USA, 2012.
[22] X. Zhang, Y. Bai, P. Hubel, Multi-Illuminant Color Matrix Representation and Interpolation Based on Estimated White Points, Apple Inc. (Cupertino, CA US), United States, 2013.
[23] X. Zhang, Y. Bai, P. Hubel, Alleviating Dominant Color Failure in Automatic White Balance Using Histogram Trimming, Apple Inc. (Cupertino, CA, US), United States, 2013.
[24] M. Bauer, S. Polzin, D. Patzelt, Quantification of RNA degradation by semiquantitative duplex and competitive RT-PCR: a possible indicator of the age of bloodstains? Forensic Sci. Int. 138 (2003) 94–103.
[25] H. Inoue, F. Takabe, M. Iwasa, Y. Maeno, Y. Seko, A new marker for estimation of bloodstain age by high performance liquid chromatography, Forensic Sci. Int. 57 (1992) 17–27.
[26] B. Li, P. Beveridge, W.T. O'Hare, M. Islam, The estimation of the age of a blood stain using reflectance spectroscopy with a microspectrophotometer, spectral preprocessing and linear discriminant analysis, Forensic Sci. Int. 212 (2011) 198–204.

VITAE

Name Miss Alisa Yaodam

Student ID 5410220074

Educational Attainment

Degree	Name of Institution	Year of Graduation
M.SC.(Forensic Science)	Prince of Songkla University	2012- Present
B.SC. (Microbiology)	King Mongkut University of Technology Thonburi	2009-2012

Work – Position and Address

Police Forensic Science Center 10

Biology and DNA Center, Police Forensic Center 10 Office of Forensic Science Police Royal Thai Police

List of Publication and Proceeding

Phuvadol Thanakiatkrai, Alisa Yaodam, Thitika Kitpipit, Age estimation of bloodstains using smartphones and digital image analysis, Forensic Science International 233 (2013) 288-297.